Optical Signal Processing Based Radio over Fiber Systems for Increased Coverage and Capacity

By
Tayyab Mehmood
NUST201464037MSEECS61214F

Supervisor
Dr. Salman Abdul Ghafoor
Department of Electrical Engineering

A thesis submitted in partial fulfillment of the requirements for the degree of Masters of Science in Electrical Engineering (MS EE)

In
School of Electrical Engineering and Computer Science,
National University of Sciences and Technology (NUST),
Islamabad, Pakistan.

(August 2016)

Approval

It is certified that the contents and form of the thesis entitled "**Optical Signal Processing Based Radio over Fiber Systems for Increased Coverage and Capacity**" submitted by **Tayyab Mehmood** have been found satisfactory for the requirement of the degree.

Advisor: **Dr. Salman Abdul Ghafoor**
Signature: _____

Date: _____

Committee Member 1: **Dr. Arsalan Ahmad**

Signature: _____
Date: _____

Committee Member 2: **Dr. Hassaan Khaliq**

Signature: _____
Date: _____

Committee Member 3: **Dr. Rizwan Ahmad**

Signature: _____
Date: _____

Abstract

At present the information age is ruled by the Internet, where all types of businesses, entertainment industry and political change is hugely shaped and influenced by the social media and the search engines. For instance, the worldwide introduction of smart-phones, Tablet PCs and the cloud paradigms for computing and data storage has directed more and more subscribers to require Internet connection (Wi-Fi, 4G) wirelessly. Large coverage and capacity, online connectivity and high mobility requirements can be fullfilled by exploiting the benefits of both millimeter-wave (mm-wave) frequencies and optical fibers. Optical fiber communication systems offer long-haul and high bandwidth transmission and the use of mm-wave frequencies provides huge bandwidth in the wireless domain. To achieve the distribution of mm-wave signals in distributed antenna system (DAS) architecture a considerable attention has been dedicated to the transmission of radio frequency (RF) signals through optical fiber systems. The amalgam of RF and optical fiber technologies has given the birth of radio over fiber (RoF) systems.

Since high-frequency signals travel shorter distances due to their higher path-loss, the cell sizes have to be further reduced. This reduction in cell size implies that more Radio Access Units (RAUs) are required for the increased number of cells, which are located close to each other. Additionally, signal processing is required at each RAU which increases the cost and complexity of the system. Hence, it is appropriate to have simple RAUs which are linked with a central unit (CU) in a centralized DAS architecture. All the resource management and signal processing can be jointly done at CU, where RAUs act as the basic elements of the coordinated multi-point (CoMP) architecture. In this situation, the connectivity between the CU and RAUs is done by the ROF technologies. ROF links are suitable for the transmission of high frequency radio signals over fiber because of their transparency to the type of RF signal, low attenuation and enormous bandwidth. In this thesis ROF based communication system has been investigated.

Dedication

I dedicate this thesis to my father for making me who I am and whom I still miss everyday.

Certificate of Originality

I hereby declare that this submission is my own work and to the best of my knowledge it contains no materials previously published or written by another person, nor material which to a substantial extent has been accepted for the award of any degree or diploma at NUST SEECS or at any other educational institute, except where due acknowledgement has been made in the thesis. Any contribution made to the research by others, with whom I have worked at NUST SEECS or elsewhere, is explicitly acknowledged in the thesis.

I also declare that the intellectual content of this thesis is the product of my own work, except for the assistance from others in the project's design and conception or in style, presentation and linguistics which has been acknowledged.

Author Name: **Tayyab Mehmood**
Signature: _____

Acknowledgment

I would first like to express my sincere gratitude to my supervisor Dr. Salman Abdul Ghafoor for his continuous support and guidance during research and writing of this thesis, for his patience and enthusiasm. I could not have imagined having a better mentor and supervisor for my Masters study than Dr. Salman.

Besides my supervisor, I would like to thank my mother for her love and prayers. I would also like to thank my elder brother for his guidance and support throughout this journey.

Table of Contents

List of Figures

List of Tables

Chapter 1

Introduction

1.1 Motivation

The exponential growth in the wireless communication technology in the last decade has brought the high bandwidth wireless connectivity to the mobile users. The uplifting volume of the Internet traffic is expected to boost the capacity of wireless channel in the coming next few years with main services like data transfer, file sharing, gaming, high quality audio and video calling and live HD streaming [5], [6]. More than 70% of the total traffic is took by the video streaming, video conferencing, and other video services and it is projected to rise at a very high annual growth rate [5]. In the upcoming years, the mobile users shall have the ability to get all the services and applications on their devices which are presently received only by the wired networks.

Currently, in the field of Photonics most of the research is focused on the optical signal processing techniques used to decrease the cost and enhance of functionalities of photonic networks. Techniques such as the use of advanced modulation formats, are in the past only used in the research domain of wireless communication are now being adopted by the optical communication systems [7]. Current advancement in photonic integrated circuits (PICs) permits the optical devices (such as laser diodes, optical splitters, optical couplers, modulators, and photo-detectors) to integrate on the same chip [8]. PIC-based optical transmitters and optical receivers are already been fabricated and installed in the public areas for fiber wireless networks [9]. These enhancements permit us to visualize that in the future optical devices such as transmitters and receivers will progressively adopt the functionalities of optical radio frequency (RF) processing and reveal the research potential of radio over fiber (RoF) systems.

1.2 Contributions

Chapter five discusses the novel contributions of this thesis, which shows the feasibility of duplex cost-effective AROF system by employing optical signal processing methods. The main contributions of the thesis are as follows:

- The proposed DAS architecture is capable of transmitting two SCM DPSK mm-wave signals to four different RAUs in the downlink.
- A single CW laser source is used at CU for the purpose of transmitting (and receiving) mm-wave signals to (and from) the four different RAUs.
- A single local oscillator (LO) of frequency 12.5 GHz is used at CU to generate eight coherent optical carriers of frequency spacing (Δf) 25 GHz.
- OCS technique is used at DD-MZM and degenerate FWM is used in the HNL-DSF fiber for the purpose of generating multiple optical carriers of spacing (Δf) 25 GHz.
- Remote Heterodyne Detection (RHD) technique is used at each RAU to achieve 25 GHz RF signals.
- In the uplink direction RAU-CU, the optical carrier of frequency (f_0) is intensity modulated with the received 25 GHz RF data signal. Only a SSB of frequency ($f_0 - 25GHz$) of the intensity modulated optical carrier is sent towards the CU.

1.3 Structure of the Thesis

One of the main type of ROF communication systems known as Analogue ROF (AROF) is discussed in this thesis. In AROF systems, RF signals are directly modulated on the optical signal.

In the *first chapter*, the motivation behind this thesis, novel contributions of the report and structure of the report are discussed in detail.

In the *second chapter*, the working principle of all the components used in our proposed ROF communication system is discussed. These components include Continuous Wave (CW) Semiconductor Laser, single-drive MZM,

dual-drive MZM, optical fiber based communication medium, EDFA amplifier, photo-detector, optical filters and the optical couplers.

In the *third chapter*, the brief introduction of ROF communication systems is discussed. Main type of ROF systems which are AROF, BROF and DROF are discussed. Performance enhancing techniques for the ROF communication systems such as optical carrier suppression (OCS) and remote heterodyne detection (RHD) are discussed. In the end of the third chapter, different types of noises in the mm-wave ROF links are discussed.

In the *forth chapter*, the literature review of ROF base cost reduction is done, where various techniques for wavelength reuse and reduction in the number of lasers are discussed.

In the *fifth chapter*, we demonstrate the feasibility of transmitting 2 SCM DPSK AROF signals in a DAS architecture employing a single LD at CU. The proposed scheme is capable of transmitting two AROF signals to four different RAUS in a duplex manner, simultaneously.

Finally, the *sixth chapter* concluded the thesis work and also highlights a number of novel ideas for the future work.

Chapter 2

Components of RoF Communication System

2.1 Optical Transmitter

The most important component of an optical transmitter is a light source. In radio over fiber communication systems, the optical source is usually considered to be an active component. The basic function of an optical source is to convert an electrical signal into an optical signal in an effective way. This phenomenon is known as the EO conversion. There are two main types of optical source available. Which are:

- Mono-chromatic Coherent Source (Laser)
- Mono-chromatic Incoherent Source (LED)

Lasers are employed as optical transmitters as well as to pump both Raman and Erbium-doped fiber amplifiers. For the long distance optical communication, semiconductor lasers are usually used as an optical source for EO conversion. They have the advantages of small size, cost-effective, energy efficient and good spectral response [3]. The basic structure and operating principle of semiconductor lasers is discussed in section 2.1.1.

2.1.1 Continous Wave (CW) Semiconductor Laser

A LASER (light amplification of simulated emission of radiation) is basically an optical amplifier bounded within a reflective cavity which forces it to oscillate through positive feedback [10]. Fiber lasers usually employ Erbium-doped fiber as the gain medium, while the semiconductor Lasers employ

semiconductor material as the gain medium. Semiconductor Lasers are noticeably the most popular optical sources for RoF communication systems. The working principle of semiconductor Laser is discussed in section 2.1.1.

Principle of Operation

A Laser works on the principle of stimulated emission. In the process of stimulated emission the excited electrons present in the higher energy state are stimulated by an incident photons, as shown in Figure 2.1. Because of the stimulated emission of photons, the electrons present in the higher energy states emits the copy of photons of same frequency, phase and direction as of the impinging photons and as a result the excited electrons falls to the lower energy state. As shown in the Figure 2.2, a laser source consisted of three main elements named as the pumping process, optical feedback mechanism and the gain medium. The gain medium which comprises of a huge amount of molecules, atoms or ions is constantly pumped by external energy source with the purpose of exciting the electrons. The external voltage applied to a Laser source is responsible for pumping which stimulates the electrons such that they goes to higher energy states and this phenomenon is usually identified as population inversion. In the laser cavity the oscillation of photons begin after the process of stimulated emission, as shown in Figure 2.2.

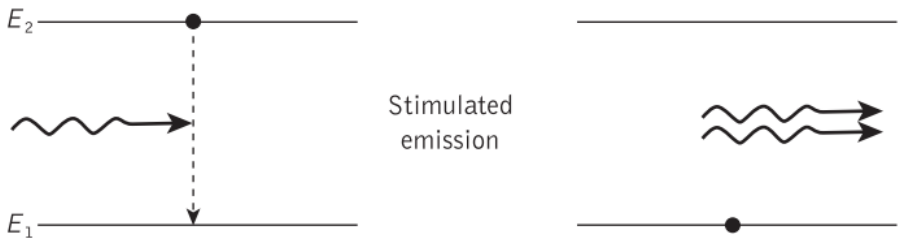

Figure 2.1: Energy state diagram for stimulated emission. The energy level of the electron is shown before and after the transition by the black dot, adopted from [1]

Further consider that the reflectors or two end of the cavity are parallel and plane and the amplifying medium is placed between these two reflectors. These reflectors are also known as the facets which work as mirrors. The laser cavity offers a feedback mechanism in which the most part of optical energy or photons are reflecting back into the cavity or gain medium, as seen in Figure 2.2.

The Figure 2.2 shows that the left facet has the reflectivity of 100% and the right side facet has the reflectivity of 80% which partially reflects back.

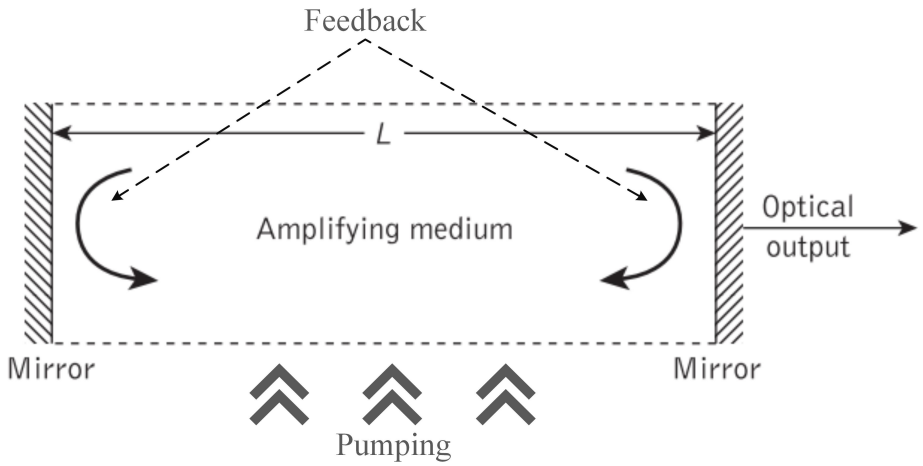

Figure 2.2: The operating principle of Laser diode, adopted from [2]

During the reflection of the photons from the facets some of the photons escape from the right side facet of the cavity and hence reflectivity is reduced. The photons escaped from the partially reflected facets are responsible for producing the coherent optical carrier at a specific frequency f or wavelength which depends on the energy difference between the energy state E_2 and the energy state E_1 of a specific material used as a gain medium. The energy difference E can be expressed as [1]:

$$E = E_2 - E_1 = hf \tag{2.1}$$

Where $h = 6.626 \times 10^{-34} j$ is a Plank's constant. A part of excited electrons in the higher energy state falls to the lower energy level after a small amount of time and give rise to spontaneous emission of photons with random phase and frequency. These spontaneously emitted photons are a source of noise in laser diodes. For a laser source to continuously produce the coherent light, the rate of stimulated emission of photons represented by R_{sti} should be higher than the rate of spontaneous emission of photons represented as R_{spo} . The following relation can be mathematically written as [3]:

$$\frac{R_{sti}}{R_{spo}} = \exp(\frac{hf}{k_B T} - 1)^{-1} \gg 1 \tag{2.2}$$

Where k_b is a Boltzman constant and T is the absolute temperature. A p-n junction is fabricated when the n-type and p-type materials are taken closer to each other, as shown in Figure 2.3 . The free holes and electrons are diffused across the both sides of the junction and the process of diffusion

continues until the equilibrium state is achieved. At the equilibrium state, the process of diffusion is stopped and because of the presence of oppositely charged holes and electrons on the both sides of the junction a strong electric field is existed.

When the voltage is applied to the p-n junction semiconductor Laser diode, the electrical field across the junction is decreases and as a result the diffusion of holes and electrons started across the junction. Whenever an electron passes the p-n junction and diffuses into a hole, it emits energy in the shape of light. The wavelength of the optical carrier depends upon the electric field strength applied across the p-n junction that can be controlled by the type of doping material used in p-type and n-type material. Alike all other semiconductor devices, laser diodes also produce noise, that is generally known as the Relative Intensity Noise (RIN). The RIN is a collection of the noise because of the alteration of frequency, phase and intensity of the emitted light. The electron-hole combination and the spontaneous emission of photons are the main reason of Relative Intensity Noise. Again, the electron-hole combination is also known as the Shot noise which is occurred in semiconductor materials due to the filling of holes with electrons.

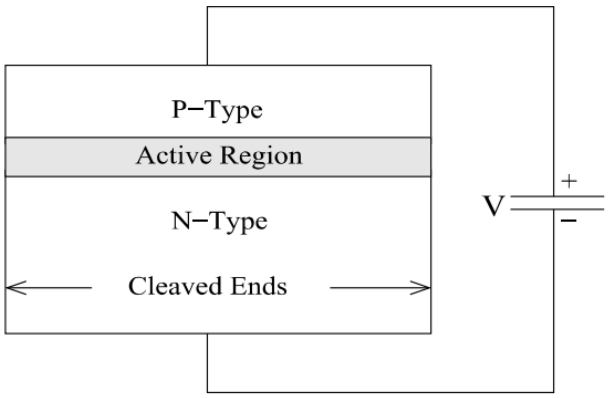

Figure 2.3: The basic structure of Laser diode, adopted from [2]

2.1.2 External Modulators

Even though the directly modulated (DM) semiconductor lasers has the advantages of low-cost and low-complexity for the generation of intensity modulated optical carriers with the limitation of low-frequency (2 GHz) modulating electrical signals. In the case of directly modulated (DM) semiconductor lasers the RIN increases with the increase in the frequencies which are closer

to the laser's relaxation resonance frequency [11]. Because of this the variations in the phase of the optical carriers increases and this effect is known as phase noise [12]. We can define group delay and the dispersion parameter as the first derivative and the second derivative of the optical phase w.r.t optical frequency, respectively. As a result, when the optical signals traveling through the dispersive optical fiber the phase noise of the optical carrier will consequence in different group velocities. Thus, the fluctuations in the group velocities will consequence in the intensity modulation (IM) of the optical carriers [13]. With the aim of reducing the impairments imposed by DM of semiconductor laser, external modulators are used for high frequency modulating signals. In Section 2.1.2 and 2.1.2 two main types of external modulators are discussed.

Mach-Zehnder Modulator

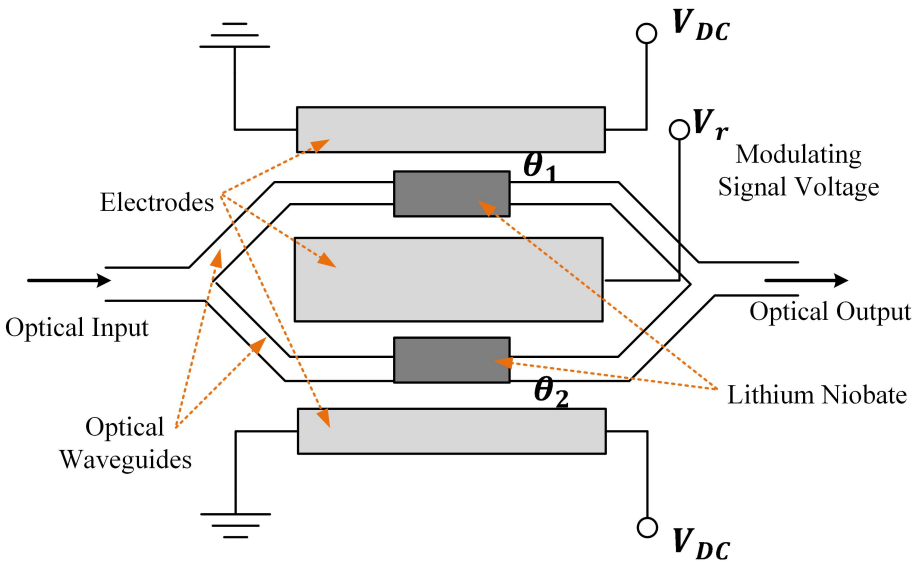

Figure 2.4: Single drive Mach-Zehnder Modulator using Lithium Niobate phase modulator in the upper and lower waveguides of a Mach-Zehnder Interferometer

MZM is one of the most commercially available optical modulator [3]. The basic structure of a single-drive MZM is represented in Figure 2.4, that is similar to the Mach-Zehnder Interferometer (MZI). When the optical carrier is applied to the single-drive MZM, it is split into path 1 waveguide and path 2 wave guide with the help of optical splitter, as demonstrated in Figure 2.4. In the beginning, the optical carriers in path 1 and 2 have same phase ϕ_1 and

ϕ_2, hence, $\phi - \phi = 0$ as seen in Figure 2.4. Each waveguide is surrounded by the electrodes and these electrodes are connected with the bias voltage V_{DC} and the modulating voltage V_r, as shown in Figure 2.4.. Both these voltages are employed to alter the phase of the optical carriers in path 1 and 2 with the help of linear electro-optic (EO) effect [11]. The EO effect is usually occurs in the non-linear mediums for example the optical crystals, where the applied electric field is responsible to change the refractive index of the crystal. When the optical signal is travelled through this kind of material, its phase is modulated because of the variations in the refractive index occurred by the amplitude variations of the applied modulating voltage across the electrodes. As shown in Figure 2.4, when the modulating voltage is not present then the DC bias voltages retain the refractive index of the materials in such a way that where will be no phase variation is occurred on the optical signals passing through path 1 and 2. When the modulating voltage is applied to the electrodes then the phase of the optical carriers travelling through path 1 and 2 varies according to the amplitude variations of the applied modulating voltage. After passing through the electrodes, the phase-modulated optical carriers from path 1 and path 2 are supper imposed by using the optical coupler as shown in the Figure 2.4. The amplitude of the resultant optical carriers is depend on the phase difference between the optical carriers traveling through both arms.

Therefore the phase variations in the optical carriers passing through path 1 and path 2 can be achieved by the amplitude variations of the modulating high frequency electric signal. The difference in the phase of the optical carriers of path 1 and 2 results the amplitude variation of the optical carriers at the output of the modulator. Same modulating voltage V_r is applied across both arms (path 1 and path 2) and therefore this type of optical modulator is known as single-drive MZM. Lithium Niobate is the most widely employed nonlinear optical crystal for the making of Mach-Zehnder Modulator [14]. The popularity of this non-linear crystal is due to its ability to function at very high frequency, high coupling efficiency with the optical fibers and induced a very small amount of chirp in the optical carriers [15]. The optical power at the output of the single drive MZM can be written in terms of optical input power as:

$$P_o = P_i \times \cos_2[\Delta\phi(t)] \tag{2.3}$$

Where $P_o(t)$, $P_i(t)$ and $\phi(t)$ are the optical output power, optical input power and the phase difference between the optical signals of path and path 2 of the MZM, as shown in Figure 2.4. The total phase difference between the optical signals of two arms can be defined as:

$$\Delta\phi(t) = \frac{\phi_1(t) - \phi_2(t)}{2} \tag{2.4}$$

Where ϕ_1 and ϕ_2 are the phase difference of waveguide 1 and waveguide 2 of single-drive MZM because of the applied modulating voltage, as shown in Figure 2.4.

Dual-Drive Mach-Zehnder Modulator

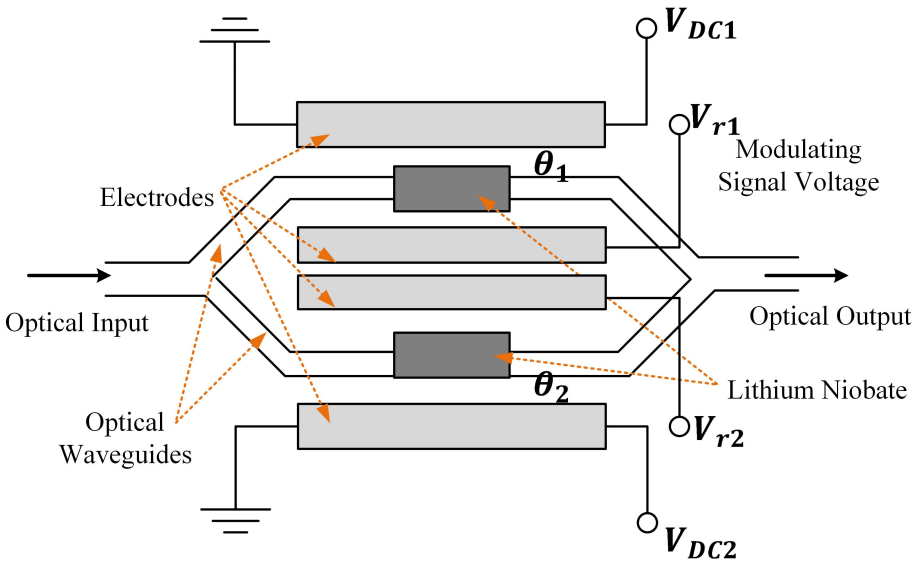

Figure 2.5: DD-MZM using Lithium Niobate phase modulator in the upper and lower waveguides of a Mach-Zehnder Interferometer along with the different modulating voltages are applied to the electrodes.

As compared to the single-drive MZM as shown in Figure 2.4, DD-MZM permits the application of different voltages denoted by V_{r1} and V_{r2} which are the voltages of upper waveguide and lower waveguide respectively, as shown in Figure 2.5. It can be seen from the structural diagram of DD-MZM which isolate the electrodes for the RF applying signals and DC bias voltage [16]. This application of DD-MZM permits the independency of the phase shifts for both optical carriers in the waveguides of the DD-MZM. As an advantage, this kind of optical modulator can be used to generate different kinds of modulated optical signals, for example Single-Side-Band (SSB) Modulation [17]. The SSB modulation is attained by applying an appropriate DC voltage V_{DC} to one of the DC electrodes, whereas all other DC electrode are grounded. Similarly, RF signals are applied to two of the

electrodes by splitting the same RF signal using electrical splitter and shifted the phase of one of the splitted RF signal by ϕ, as seen in Figure 2.5.

The output optical field $E_{MZM}(t)$ of a dual-drive MZM can be mathematically written as:

$$E_{dual}(t) = \frac{1}{2}\left[e^{j\left(\frac{\pi V_{DC1}}{V_\pi}+\frac{\pi V_{r1}(t)}{V_\pi}\right)} + e^{j\left(\frac{\pi V_{DC2}}{V_\pi}+\frac{\pi V_{r2}(t)}{V_\pi}\right)}\right]\sqrt{2P_{\text{in}}}e^{j\omega_c t} \tag{2.5}$$

Where the bias voltage $V_{bias} = (V_{DC1} - V_{DC2})$ is differentially applied to both arms of DD-MZM through voltages V_{DC1} and V_{DC2}. The modulating voltage $V_t = (V_{r1}(t) - V_{r1}(t))$ is also differentially applied to both arms of DD-MZM through voltages $V_{r1}(t)$ and $V_{r2}(t)$.

Here, V_π is the switching voltage needed to alter the phase of the propagating signal by π radians, f_c is the central frequency of the applying optical carrier and P_{in} is the power of the feeding optical signal which is generated by the laser diode. The intensity of the optical carrier at the output of the DD-MZM can be mathematically written as by using 2.5:

$$P_{dual}(t) = P_{\text{in}}\left[1 + \cos\left(\frac{\pi V_{bias}}{V_\pi} + \frac{\pi V(t)}{V_\pi}\right)\right] \tag{2.6}$$

2.2 Optical Fiber

In optical communication systems, the most widely used transmission medium is Optical fiber. Optical fiber works on the basic phenomenon of Total Internal Reflection (TIR). When the optical signal enters the fiber core at some specific angle it remains restricted to the optical fiber core due to phenomenon of TIR. The reflection of light occurs at the boundaries of the fiber core because of the significant difference in the refractive indexes of the core and cladding of optical fibers. The refractive index of the core section is significantly higher as compared to the cladding section. As shown in Figure 2.6, the optical fiber comprises of two main sections, the outer cladding section and the inner core section. It has cylindrical shape and made up of silicon material [18].

In this report, we will only discuss the most widely used type of optical fiber, named as single-mode fiber (SMF), as seen in Figure 2.6. It is stated as the single mode because this kind of optical fiber permits just one mode of light to pass through it. As compared to the radius of the cladding section, the core has small radius. The single mode of light pass through the core in a straight path without any reflections from the boundaries of the core if the

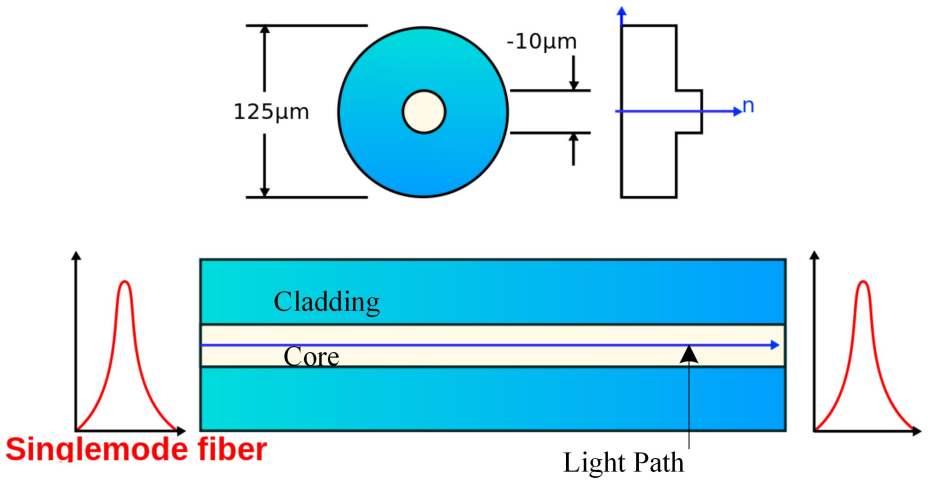

Figure 2.6: Basic Structure of Single Mode Fiber, adopted from [1]

size of the core section radius is on the order of the wavelength of light being used [3].

The refractive index profile of SMF is shown in Figure 2.6 usually follows a step-index profile. The typical SMF has a cladding diameter of 125μ And the core diameter of 10μ. Because of the comparable core radius of SMF the wavelength of light, the TIR is no more responsible for the confinement of light in the SMF core.

Instead of TIR, the step variation in the refractive index of core and cladding section of SMF supports in restricting the light into the fiber core. In an optical fiber medium which has a homogeneous refractive index, the spreading of the wavelength of optical signal is due to the phenomenon of diffraction [18].

As a result, the beam width of the optical signal passing through the homogeneous medium will rise, but luckily the beam width of the optical signal can be controlled by sensibly scheming the refractive index profile of the transmission medium. We can control the beam width of the optical carrier passing through the fiber by keeping the refractive index of the transmission medium high near to the center of the core as related to the edge of the core and as a result the light travels slower at the center of the core than the edge of the core.

The reduction in the speed of optical signal at the center of the core as compared to the speed of the light at the periphery permits the transmission medium to keep the light signal focused, by stopping it from increasing. Like other transmission mediums, when the data carrying signal passes through

the optical fiber medium it executes impairments on that signal, that contain non-linearity, attenuation and dispersion. In section 2.2.1, 2.2.2 and 2.2.3 all these kinds of impairments are discussed in details.

2.2.1 Fiber Attenuation

When the optical signal is travelling through the optical fiber, optical fiber attenuates it. The two basic reasons for the attenuation of a signal in the optical fiber are:

1. Material absorption
2. Rayleigh scattering

Material absorption in optical fiber can be splitted into two further categories which are as follows:

- Intrinsic absorption
- Extrinsic absorption

The former type of material absorption is because of silica itself, which is employed to make the optical fiber. While the later type of material absorption is because of the impurities in silica [1].

Rayleigh scattering is the second main reason of attenuation in optical fibers and it is occurred inside the core of the fiber because of the variations in the refractive index [1]. Each time the variation in refractive index varies the light is reflected back and because of this reflection the light is not received at the receiver. The attenuation happened due to rayleigh scattering is significantly higher than the material absorption. Rayleigh scattering is inversely related to the forth power of the wavelength of the optical signal, as shown in Figure 2.7.

The attenuation α of the optical fiber can be mathematically represented as:

$$\alpha = \frac{10}{L} \log_{10}(\frac{P_{out}}{P_{in}}) \tag{2.7}$$

Where, L is the length of fiber, P_{out} and P_{in} are the output and the input optical power of the optical fiber. The overall attenuation of the fiber in the $1.3\mu m$ and $1.5\mu m$ bands is as low as $0.2dB/km$.

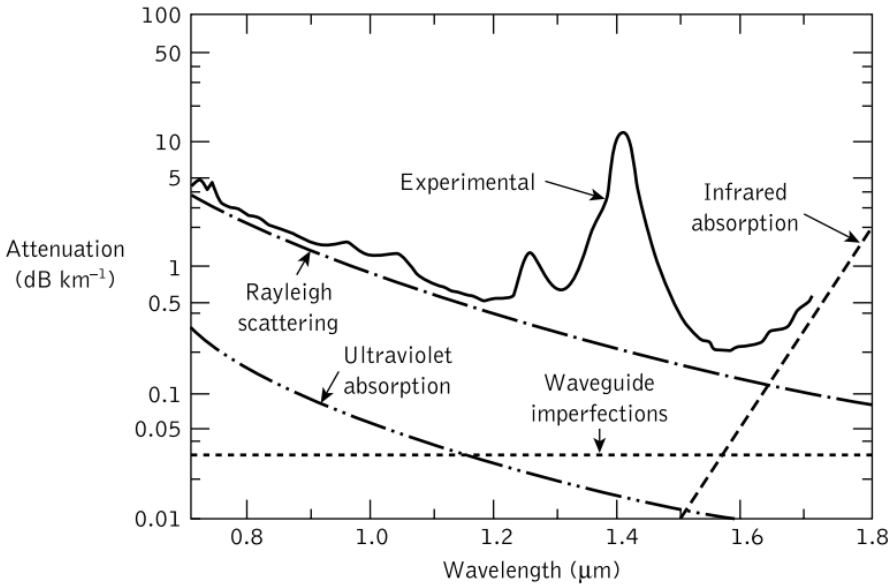

Figure 2.7: Optical fiber attenuation vs wavelength, adopted from [1]

2.2.2 Fiber Dispersion

In the phenomenon of fiber dispersion the light of different wavelengths travels at different speeds within the optical fiber core and this is because of the wavelength-dependent refractive index of silica. As we know that the optical signal (either pulsed or CW) is composed of infinite range of wavelengths. Hence because of the refractive index variations each wavelength travels at different speed [15].

Chromatic dispersion occurs in the core of the optical fiber when the different spectral components of light pulse travels at different velocities. it is occurred because of the following two resows:

1. Material dispersion

2. Waveguide dispersion

Material dispersion is because of the frequency-dependent refractive index of silica (material used to make the fiber). Hence different spectral components travels at different speed in silica based fiber [15]. Waveguide dispersion arises due to the wavelength-dependent propagation constant of fiber. As the wavelength of the optical signal increses, the fundamental mode is spread from core to cladding and as a resultant the fundamental mode travels faster, as shown in Figure 2.8.

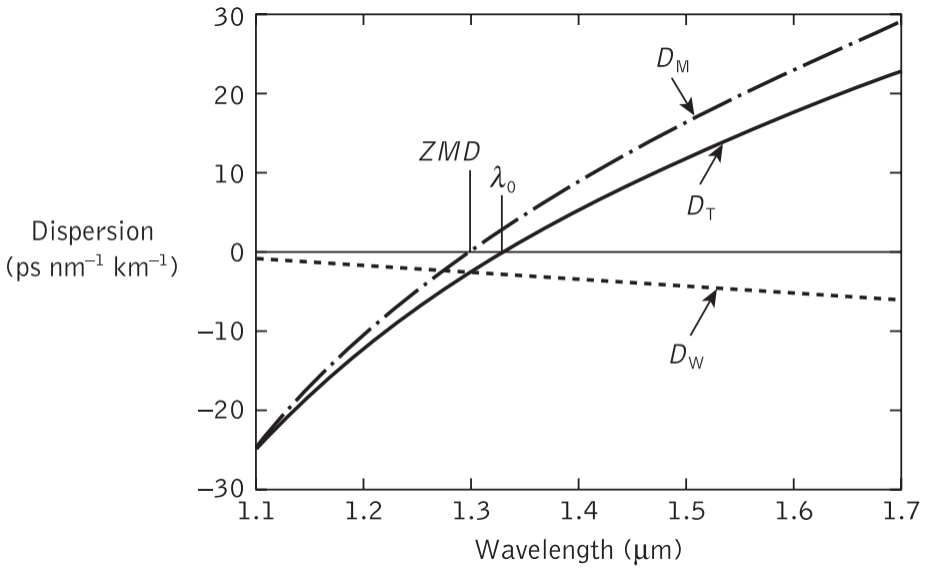

Figure 2.8: Optical fiber Dispersion vs wavelength, adopted from [1]

2.2.3 Fiber Non-linearity

Just like any dielectric mediums, by rising the intensity of the optical signal travelling through fiber from a specific threshold the behavior of the optical fiber medium becomes non-linear. The nonlinear parameter γ is used to quantify the nonlinearity of the optical fiber and it can be mathematically written as:

$$\gamma = \frac{n_2 \omega_o}{c A_{eff}} \tag{2.8}$$

Where ω_0 is the frequency of optical carrier, c is the speed of light in vacuum, n_2 is the nonlinearity index of optical fiber and A_{eff} is the effective area of the fiber core section [19].

As shown in Figure 2.8, the nonlinear parameter can be altered by altering the effective area of the core A_{eff} or the non-linear index of the fiber n_2. Non-linear index of the fiber n_2 is dependent on the material of the optical fiber core and can be controlled by adjusting the quantity of impurities in silica. Generally because of the nonlinearity of the optical the harmonics of the optical input signal into the fiber generated and as a result the spectrum of the optical carrier broadened [20]. When the optical carrier with finite spectral bandwidth passing through the optical fiber, the nonlinearity of the optical fiber also affects the phase of each spectral component. The change in the phase of the spectral components results in the generation of new frequencies and hence responsible for broadening the spectrum. The

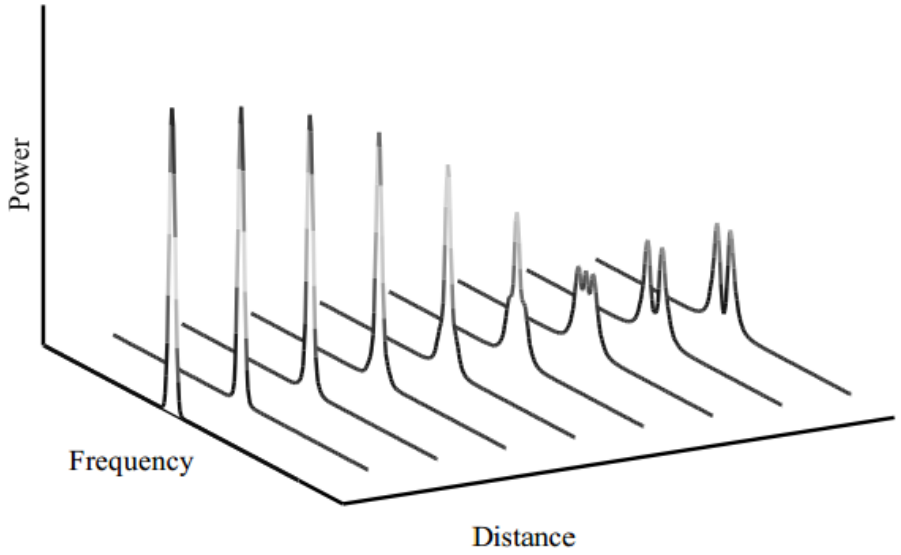

Figure 2.9: Optical fiber Dispersion vs wavelength, adopted from [2]

spectral broadening due to the nonlinearity of the optical fiber can be controlled by controlling the power of the optical signal. The phenomenon of spectral broadening is illustrated in Figure 2.9, where the spectrum of the pulse broaden as the length of the fiber increases.

2.3 Optical Receiver

The job of an optical receiver is to achieve the optical to electrical (OE) signal conversion. In this section, we will briefly review the mechanism of photo-detection and the model of generally employed photo-detector (PD) named as the PIN photodiode.

2.3.1 Principle of Photodetection

Photo-detectors are a product of semiconductor materials. In the absence of light, the electrons are in the valence band of the semiconductor material. But when the light (photons) incident on the semiconductor material, the photons or energy packets are absorbed by the electrons and these electrons gain energy and move from the valence band to the conduction band of the semiconductor. Because of this process the electron-hole pair is made. When the external potential or voltage is applied in a reverse bias, the electron-hole

pair generates the flow of electric current and this kind of current is known as the photo-current [21].

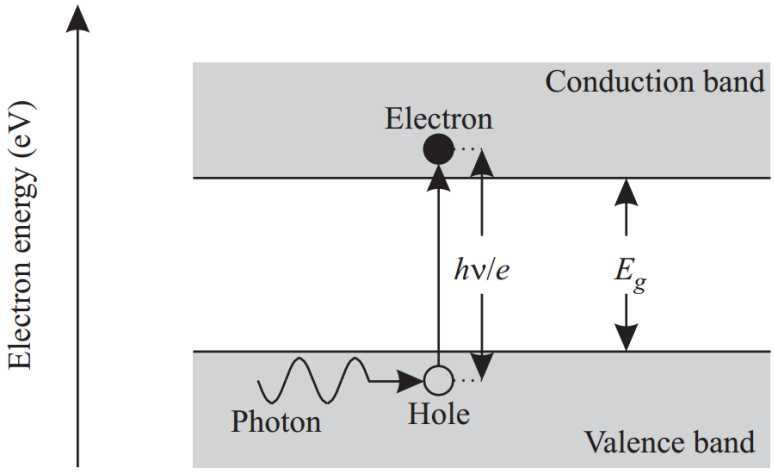

Figure 2.10: The basic principle of photodetection employing a semiconductor material, adopted from [1]

The phenomenon of photo-detection is represented in details in Figure 2.10, where a single photon is absorbed by the valence band electron and it move from the lower band to the conduction band. To get the electron transition happened from lower energy band to higher energy band, the energy of the incident photons must be equal to the energy gap or the energy difference between the conduction and valence bands as shown briefly in Figure 2.10. One of the simplest type of photo-detector is formed by combining the p-type and n-type materials together which made a p-n junction. When the photons incident on the surface of p-n junction which is connected to the external potential in a reverse bias, the electron-hole pairs are formed which flows in the reverse direction because of the applied external source.

2.3.2 PIN Diode

As we studied earlier that the photocurrent is produced because of the drifting of electrons across the depletion region but it can also be generated by the diffusion of electrons and holes [4].

Hence, when the incident light falls on the depletion region of the PD the drifting current is produced and the when the incident light falls on the p-type and n-type of the semiconductor materials in PD, the diffusion current is produced. When the holes and electrons are produced in the n-type and p-type semiconductor materials respectively, these electrons and holes

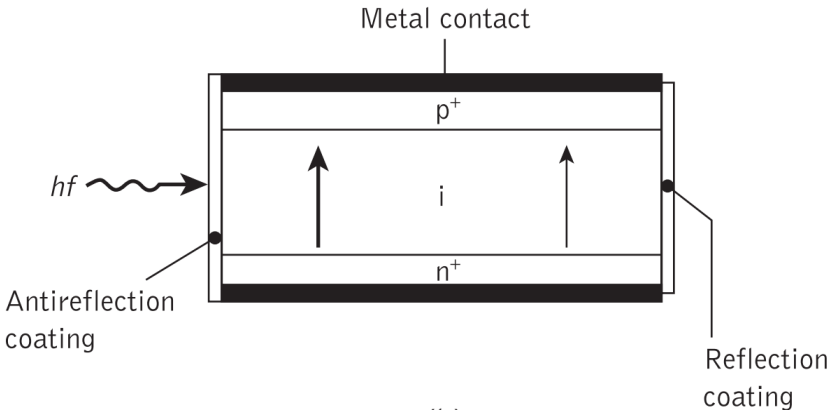

Figure 2.11: The structure of the side illuminated *pin* photodiode, adopted from [1]

are moved towards the walls of depletion region before they move towards the opposite directions. If we decrease the length of the p-type and n-type semiconductor materials then the diffusion current can be reduced. We want to reduce the diffusion current because the diffusion of electrons and holes is a slow process and hence it can delays the PD response to the rapid change in the intensity of light incident on PD. The reduction of diffusion current with the decrease in the length of p-type and n-type materials makes the drift current dominant. This can be accomplished by putting the intrinsic semiconductor material between the p-type and n-type semiconductor materials, as shown in Figure 2.12. Because of this kind of structure of photodiode, it is commonly known as the PIN photodiode where P, I and N alphabets stands for p-type, intrinsic and n-type semiconductor materials respectively, as shown in Figure 2.12.

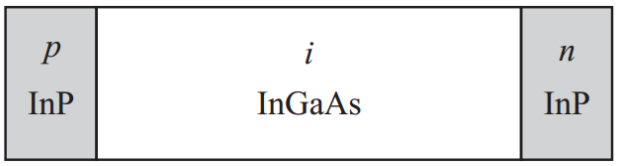

Figure 2.12: Heterostructure based *pin* photodiode

2.4 Optical Amplifiers

As discussed earlier in Section 2.2.1, the optical fiber cables attenuates the optical carriers. Additionally, in the optical network there are other passive

components used for different purposes such as optical couplers, optical splitters, add-drop multiplexers and optical filters, the insertion losses added by these components decrease the overall power of the optical signals. Hence the optical amplifiers are necessary at fixed intervals so that the overall power of the optical carriers remain suitable for the transmission of these signals from transmitter to the receiver. One of the most widely used optical amplifier in the optical fiber communication systems is the Erbium Doped Fiber Amplifier (EDFA).

2.4.1 Erbium Doped Fiber Amplifier (EDFA)

The working principle of Erbium Doped Fiber Amplifiers is similar to the working principle of laser diodes as previously discussed in Section 2.1.1. These amplifiers also use the gain medium for the purpose of pumping, in case of EDFAs the pumping medium is a small piece of Erbium Doped Fiber. Just like we discussed previously in Section 2.1.1, when the phenomenon of pumping occur, the electrons in the lower band absorb the light or energy packets and go to the higher energy state or conduction band.

All the electrons in the higher energy band are stimulated by the photons of an incoming optical signal to fall back to the conduction band or the lower-energy state, while emitting the photons which have the similar properties as of the incoming optical signal have. Hence, the freshly generated photons have the same direction of motion, frequency, phase and the polarization as of the incident photons of the incoming signal have. This phenomenon is known as stimulated emission, as previously discussed in Section 2.1.1 and because of this process the incoming optical carrier is amplified.

The wavelength of the amplifying signal depends upon the material used to dope the optical fiber. The energy gap between the higher energy state and the lower energy state depends upon the material used in optical fiber. In case of Erbium doping of fiber, we can amplify the wavelengths of range 1525 nm to 1570 nm, in these regions the attenuation attached due to fiber is minimum as shown in Figure 2.13.

Hence the Erbium ion is an appropriate dopant for the amplifying devices employed in the optical communication systems. In Erbium ion, the excited electrons have the tendency to go to multiple different energy bands but here we only let two basic energy levels termed as the higher energy levels E_3 & E_2 and the lower energy levels E_1, as shown in Figure 2.14.

As shown in Figure 2.15, the pumping laser source operating at the wavelength of 980 nm are used to pump the elections from the lower energy levels E_1 to higher energy levels E_3 and pointed by the upward arrows as shown in Figure 2.14. These kind of laser sources consumes low power while running.

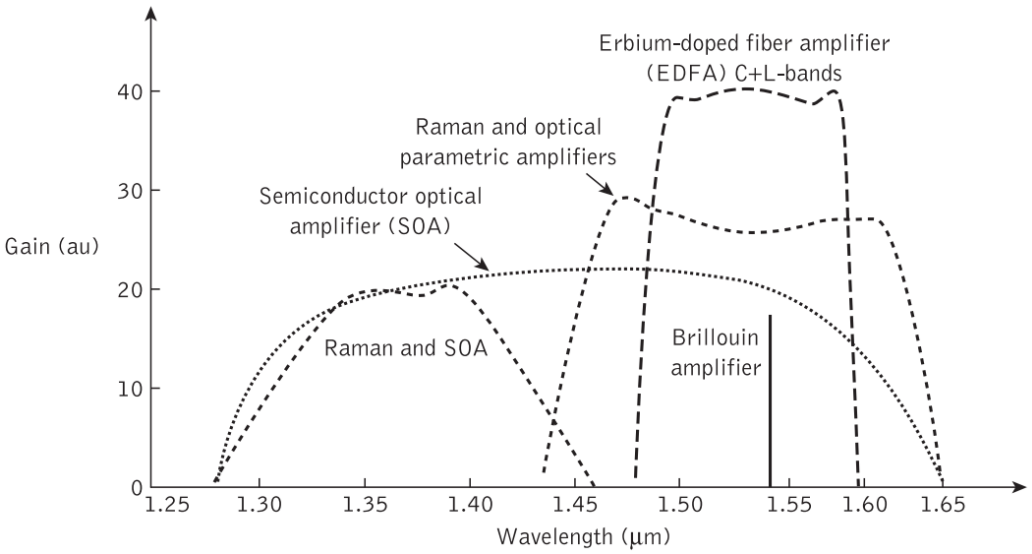

Figure 2.13: Wavelength vs Gain characteristics graph for different types of optical amplifiers, adopted from [3]

The electrons after reaching in the higher energy state E_3 spontaneously falls back to the lower energy level E_2. The transition time between E_3 energy level and E_2 energy level is too small than the transition time between E_2 energy level and E_1 energy level.

Hence the probability of amplifying the input optical signal is very high in the wavelength range of 1525 nm to 1575 nm because of the reason of electrons stays for a longer time at E_2 energy level.

The Figure 2.15 shows the basic structure of two-stage EDFA where the amplifying medium is splitted into two parts. Each of the amplifying medium is pumped by the pumping laser source of wavelength 980 nm which are coupled with the fibers directly. EDFA contains an optical isolator for the purpose of stopping the optical signal travelling in the backward directions such as because of reflections in the optical networks. The optical filter between the Erbium fibers is used to reject the noise produced in the process of amplification of the optical signal [22].

Just like the laser diodes, the optical amplifiers also produce the noise which is the reason in the reduction of output signal's OSNR. The key reason of noise in the optical amplifiers is known as Amplified Spontaneous Emissions (ASE) Noise. This kind of noise generates because of the spontaneous fall down of the electrons from the higher energy level E_3 to lower energy level E_2 with the release of a random photon whose direction, phase and polarization is random as shown in Figure 2.14.

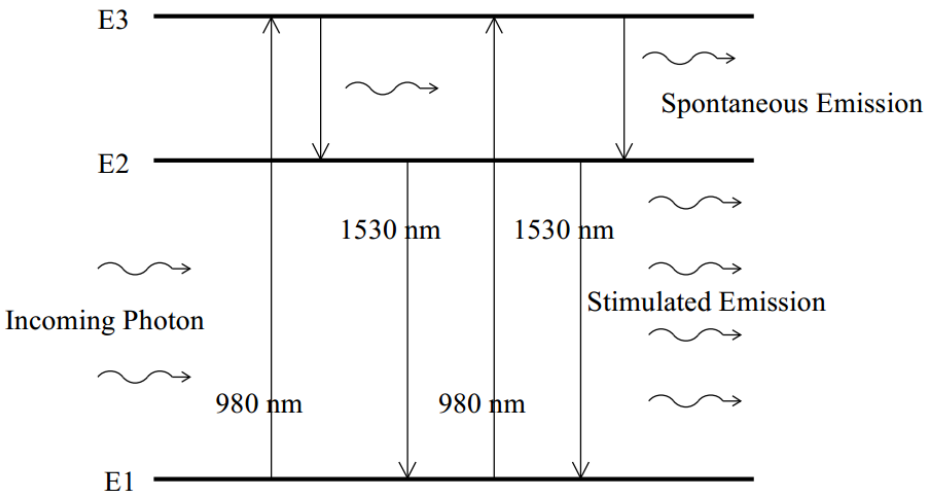

Figure 2.14: Basic phenomenon of Erbium doped fiber amplifier, adopted from [4]

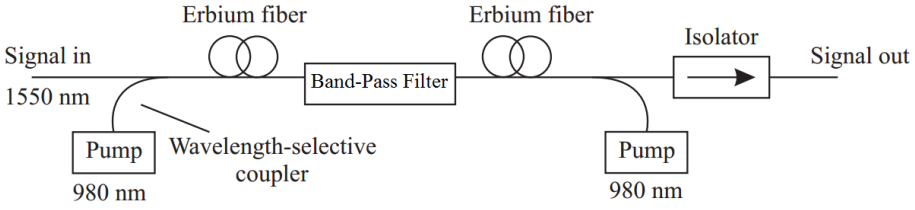

Figure 2.15: Basic structure of Erbium doped fiber amplifier, adopted from [2]

2.5 Optical Filters

Usually optical filters are used to separate a single wavelength from multiple WDM wavelengths or remove a single wavelength from multiple WDM wavelengths. These kind of filters are also useful to remove the out of band ASE noise from the examining set of signals. These kind of optical filters have the properties of low insertion loss, small size, cost-effective and temperature independent. In the next section, we will only discuss the Arrayed waveguide Grating (AWG) filters which are commonly used in the radio over fiber communication systems.

2.5.1 Arrayed Waveguide Grating Filters

To get the spatial separation or to separate out all the wavelengths of the composite signal Arrayed Waveguide Grating (AWG) filters are usually used in optical fiber communication systems. The basic model of AWG can be seen in Figure 2.16. Arrayed Waveguide Grating (AWG) filters employ optical waveguides to achieve spatial separation. AWG filters works on the basic principle of optical interferometers [23]. In order to filter out a single wavelength, the simplest type of MZI use two optical couplers (OC) which are attached to two discrete optical waveguides, similar to the operation of MZM. In the slimier manners, the AWG is consist of two OCs which are attached by more than two waveguides so that it can filter out more than two wavelengths by employing the principle mentioned and shown in Figure ??.

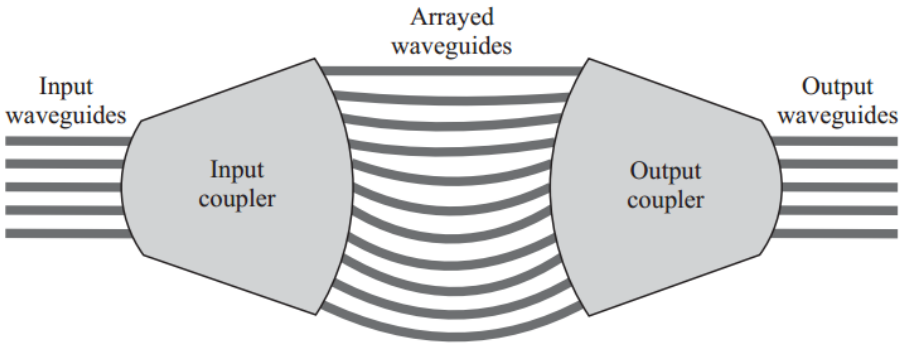

Figure 2.16: General model of Arrayed Waveguide Grating Filter, adopted from [1]

It can be seen in Figure 2.16 that the AWG comprises of a set of arrayed waveguides, input and output waveguides and two slab waveguides. The

arrayed waveguides are made up of silica material.

When the optical carrier enters into the AWG filter and via input waveguide it travels and enters into the first slab waveguide. As shown in Figure 2.16, in the first slab waveguide the input optical signal diverges in the free propagation area of the first slab waveguide. The optical signal which spreads in slab waveguide is taken by the number of arrayed waveguides that works as dispersive elements. All these arrayed waveguides are arranged in such a way that each have a constant length difference with the adjacent waveguide [24]. The length of individual waveguide is selected in such a way that a specific wavelength experiences the same dispersion in each waveguide. Hence, after passing through the free propagation area of the second slab waveguide, all the incoming lights from the multiple waveguides have their specific wavelengths which constructively concentrate their output on a specific output waveguide.

2.5.2 Optical Couplers/Splitters

The optical couplers (OC) are employed either for combining the optical signals or for splitting the optical signal, as shown in Figure 2.17. One of the most widely used type of OCs is the fused fiber coupler, as shown in Figure 2.17 which is fabricated by fusing the two fibers together [4]. When the optical fibers closed to each other and aligned in a parallel manners then the optical signal is coupled from one fiber to an other. The coupling efficiency depends upon how close these fibers are, as shown in Figure 2.17. We can control the power of the output optical signals from the two output ports by adjusting the distance between the fused fibers and also by changing the lengths of these fibers. Pair of free ends on the left side are employed as an input ports while the pair of free ends on the right side are employed as an output ports.

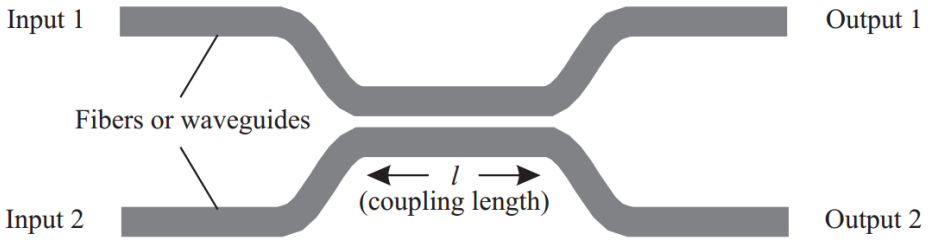

Figure 2.17: Basic structure of optical coupler, adopted from [4]

Chapter 3

Radio over Fiber Communication Systems

3.1 Radio Over Fiber Communication Basics

Radio over fiber is a kind of technology which allows the transmission of radio signals (mm-wave signals, Microwave signals or UWB signals) over fiber.

In general, the following techniques are used in radio-over-fiber systems:

- Generation of millimeter-wave Carriers
- All optical processing of millimeter-wave carriers
- Photonic distribution of millimeter-wave signals
- Optical analog-to-digital conversion

In this thesis, our main focus is on the generation of millimeter-wave (mm-wave) carrying optical carriers. Further, we will demonstrate the transmission and reception of high frequency RF signals to and from the RAUs.

The basic block diagram of radio over fiber architecture is shown in Figure 3.1, where radio signal is transparently transmitted over the lightwave path. The photo-detector is used at the receiver to detect the optical carrier signal and generate the radio signal.

Figure 3.2 and Figure 3.3 displays two different cellular architectures, Figure 3.2 shows the current cellular architecture that are established on macro-cells, however Fig. 3.3 shows the future cellular architecture that is based on a ROF backhaul links considered to support multiple small cells. The design shown in Fig. 3.2 has low signal power and low quality of service at the edge of the micro-cell. All these challenges are overcome by

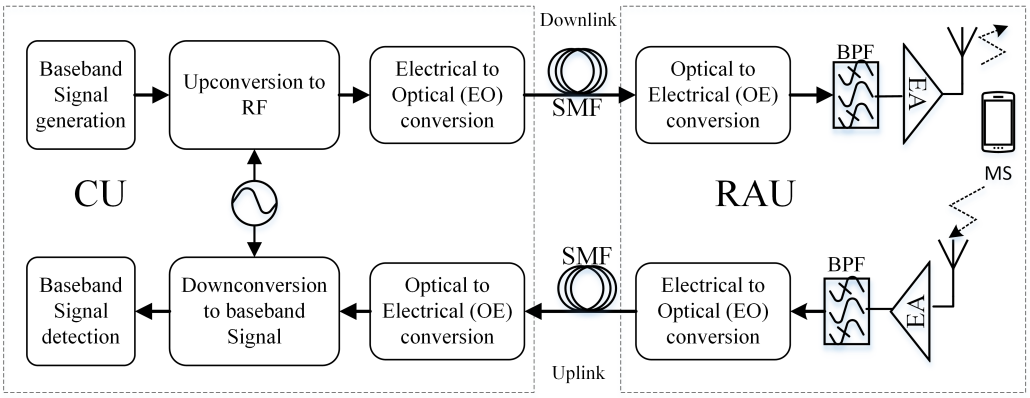

Figure 3.1: Basic block diagram of radio over fiber architecture

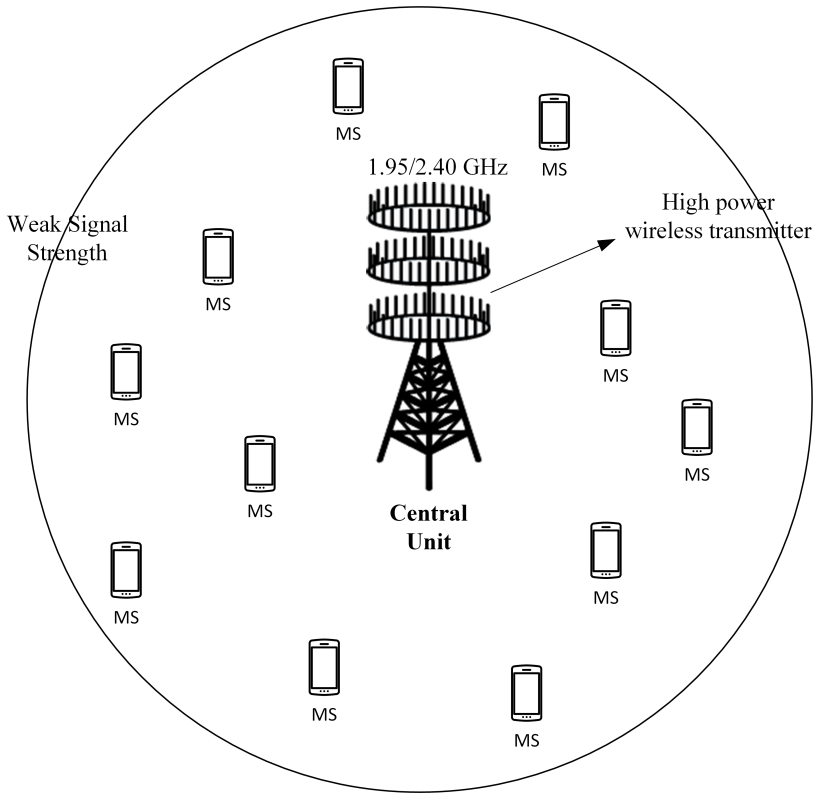

Figure 3.2: Cellular architecture without employing ROF (MS- mobile station)

using ROF link based cellular architecture which supports multiple low-cost, less-complex and smaller cells, as shown in Fig. 3.3. The main benefit of ROF link is its ability to merge the advantages of both optical and wireless communication techniques. Clearly, the benefits of the ROF systems can be describe in detail as follows [25], [26], [27].

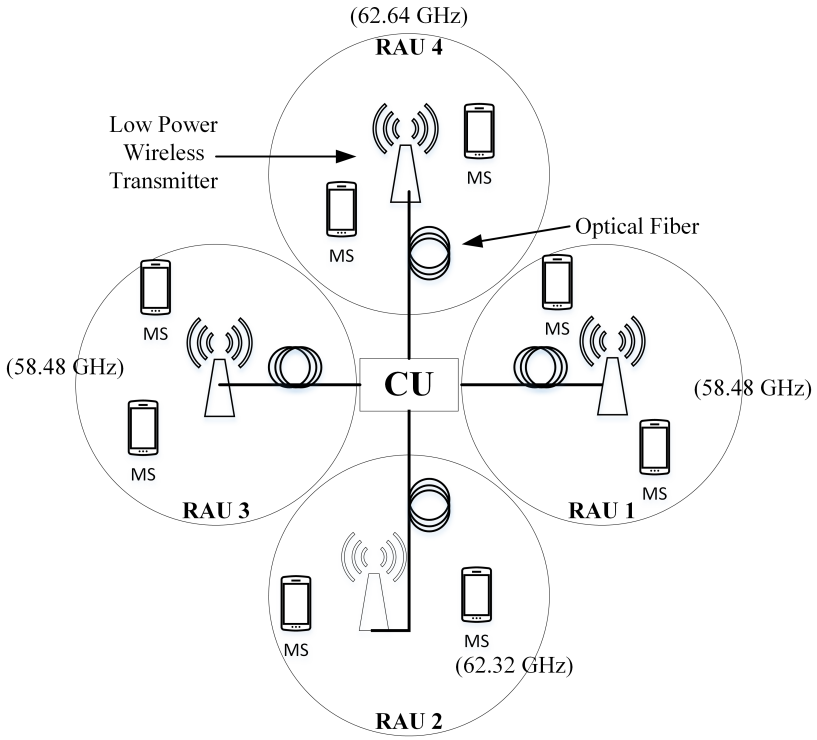

Figure 3.3: Cellular architecture using ROF (MS- mobile station; CU- central unit; RAU- radio access unit)

1. **Low attenuation of optical fiber:** Low loss optical fiber (0.2 dB/Km) cables efficiently accelerates the establishment of huge number of geographically distributed antennas which are connected to the CU. The Distributed Antenna System (DAS) [28] architecture is shown in Figure 3.3. Four RAus are connected to the central unit in a star-like architecture through optical fiber. Each CU has the ability to support a huge number of RAUs through optical links.

2. **Economically feasible small cell based Cellular architecture** In ROF based communication system, each CU assists a number of RAUs as shown in Figure 3.3, where resource management and signal processing tasks of each RAU is jointly done at the CU. Hence, RAUs

become simple and low-cost and the overall cost of setting up small cells based cellular architecture is reduced [29]. Furthermore, the centralization of signal processing tasks of all the RAUs that take place at CU guarantees the ease of up-gradation in the hardware as well as in technology which can be possible by using coordinated multipoint (CoMP) architecture [30].

3. **Enormous bandwidth** The single mode fiber (SMF) is characterized by its large bandwidths and which can be discussed using the suitable schemes presented in this article.

4. **Energy Efficiency** With the deployment of smaller cells the distance between the RAU antenna and the mobile user decreases which gives the strong signal strength at the mobile user end, as shown in Figure 3.3 and hence the path loss decreases too. Because of the smaller cell size,the required power for the antenna terminals at each RAU is reduced and because of this inter-cell interference (ICI) is reduced too [31].

5. **Possibility to apply MIMO techniques [32]** In wireless communication the techniques which uses a number of antenna terminals at the remote access unit and at the mobile device to support a single mobile subscriber are denoted to as MIMO techniques [33]. The DAS along with the CoMP algorithms are used at the central unit to enhance the overall throughput and to offer the diversity gain to the mobile user of Figure 3.3.

6. **Better coverage of wireless network** As shown in Figure 3.2, there exists a large area especially at the edge of the macro-cells in cellular architecture where the mobile users did not receive the wireless signals with enough signal strength. In ROF assisted cellular architecture the region of these low-signal-strength signals is minimized, as shown in Figure 3.3.

3.1.1 Types of RoF Systems

According to the different types of modulating signals which are modulated on the optical carrier for purpose of transmitting over optical fiber channel the ROF systems can be divided into three types as shown in 3.4.

1. Analogue ROF (AROF) Systems

2. Baseband ROF (BROF) Systems

3. Digitized ROF (DROF) Systems

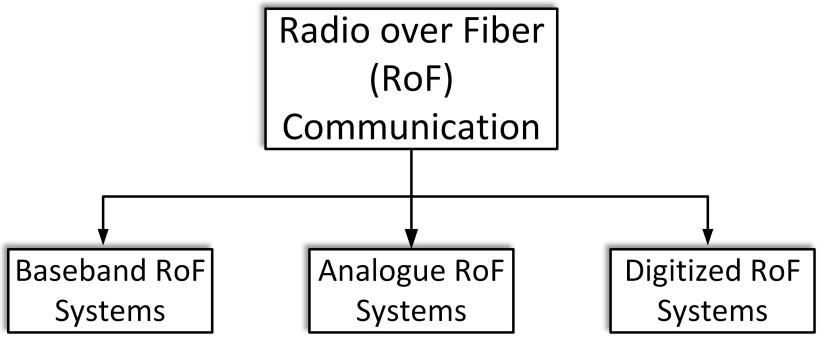

Figure 3.4: Different types of ROF architecture

Analogue ROF (AROF)Systems

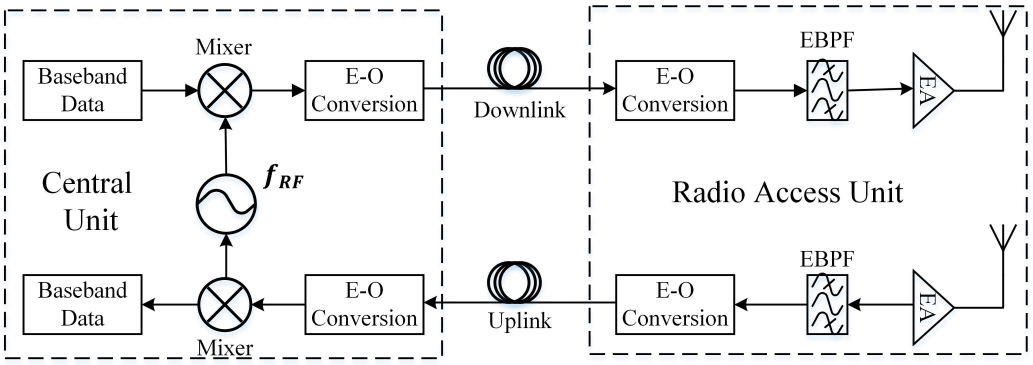

Figure 3.5: Basic architecture of AROF link (EBPF-Electrical BandPass Filter; EA-Electrical Amplifier)

It is a kind of ROF system in which digital bit streams are converted into baseband data. Then baseband data is modulated on RF carrier signals and these RF carrier signals are modulated on an optical carrier to transmit the data over optical fiber. In AROF systems, RF frequency up-conversion and carrier modulation is done at central unit (CU). At the transmitter side, RF signal is up-converted with the help of E/O up convertor (MZM) while photo-detector or down-converter is used at the receiver side to get the RF signal from optical carrier [34] . The key difference between AROF architecture and BROF architecture is that the placement of local oscillator

(LO), in AROF links the up-conversion is done at the CU by using the LO while in the BROF links the up-conversion of base-band signals is done at each RAU by employing LOs. Hence, as compared to AROF systems where only a single LO is required for up-conversion, in BROF systems N number of LO are required at N RAUs. Additionally, in the DROF systems A/D conversion and D/A conversion is required which is not needed in AROF systems.

Baseband ROF (BROF)Systems

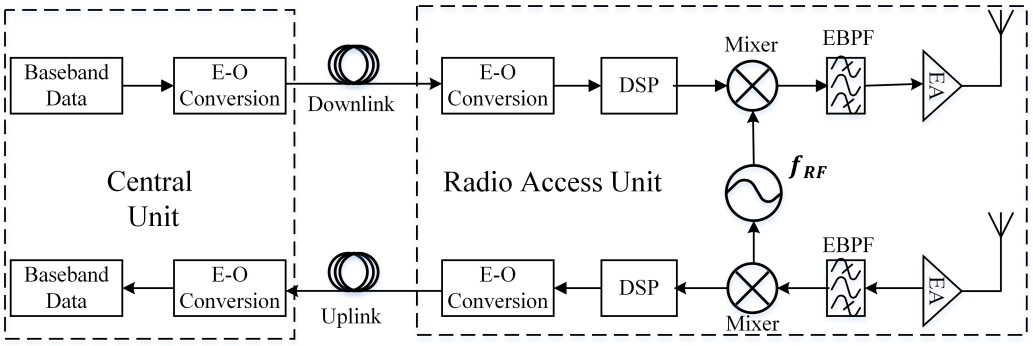

Figure 3.6: Basic architecture of BROF link (DSP-Digital Signal Processing; EBPF-Electrical Bandpass Filter; EA-Electrical Amplifier)

At the transmitter, the baseband data is directly modulated on optical carrier by using the EO converter and then transmitted over lightwave channel. At the receiver side, to get the baseband signal OE conversion is performed. To send the high frequency RF signal from the antenna baseband signal is processed and then up-converted to the high-frequency RF signal [35]. The key difference between between the BROF links and the AROF systems is the placement of LO for the purpose of up-converting the base-band signals. As compared to DROF systems, there is not need of A/D converters or D/A converters.

Digitized ROF (DROF)Systems

In this architecture of ROF system the analogue RF signal is digitized before sending the data over optical fiber. First the baseband data is converted into analogue RF signals then these RF signals are converted into binary pulses by using the analogue-to-digital converter (ADC). After this binary electronic pulses are modulated on optical carrier for the transmission over fiber [36]. By using OE converter, optical carrier is converted into the electronic pulses

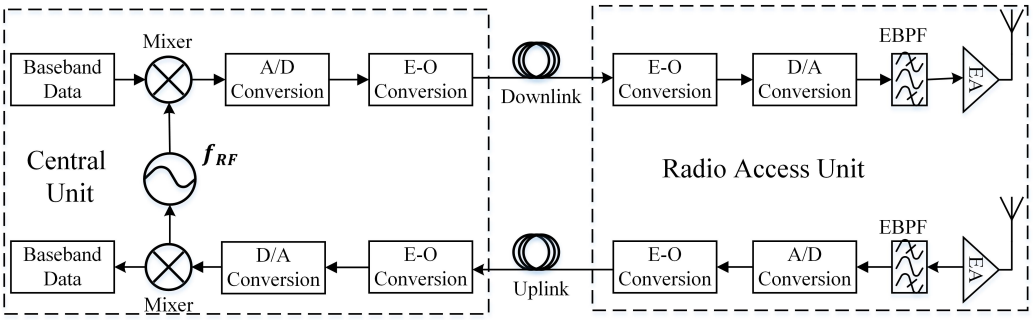

Figure 3.7: Basic architecture of DROF link (A/D Conversion-Analog to Digital Conversion; D/A Conversion-Digital to analog Conversion; EBPF-Electrical Bandpass Filter; EA-Electrical Amplifier)

at the receiver side and to get high frequency RF signals electronic pluses digital-to-analogue conversion (DAC) is performed. As compared to AROF links, DROF links are more resilient to losses because of the digital nature of the carriers passing through the optical fiber. Therefore, DROF systems performs better in the scenario where RAUs are deployed far from the CU.

3.2 Techniques for Transporting RF Signals over Fiber

In this section, we will briefly discuss the techniques used for transmitting and receiving the RF signals over fiber.

3.2.1 Intensity Modulation Combined with Direct Detection (IM/DD) Method

Intensity modulation relying on direct detection (IMDD) is one of the simplest technique used for carrying radio signals over fiber [67], [10]. In this technique, the variations in the intensity of the optical signal are directly proportional to the intensity of the radio signal we wants to transmit from CU towards RAU. Intensity modulation of the signal can be done either using direct modulation or using external modulation. We here only discuss external modulation technique in detail because direct modulation of the laser diodes is not appropriate for high frequency RF communication systems. The basic structure of external modulation based Intensity modulation relying on direct detection (IMDD) RoF system is shown in Figure 3.8. In

external modulation, the modulator is employed to modulate the intensity of an optical signal.

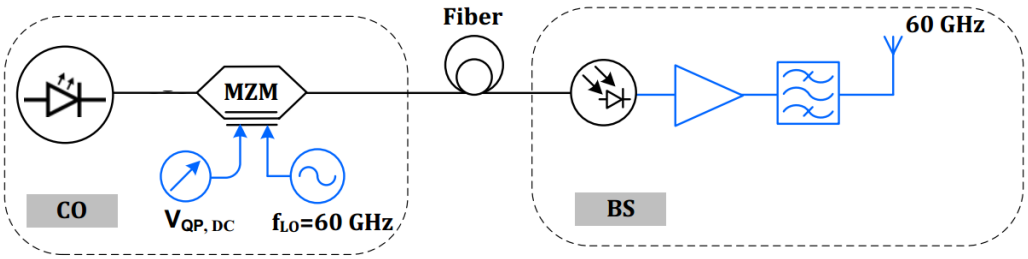

Figure 3.8: Schematic diagram for Intensity Modulation Combined with Direct Detection (IM/DD) technique

MZM is the most commonly used external modulator type in the optical communications as briefly discussed in Section 2.1.2. The working of MZM modulator is Shown in Figure 2.4. External modulator has the advantage of reducing the effect of fiber dispersion with the use of single side band (SSB) modulation of the optical carrier. But external modulators has the disadvantage of high cost as compared to the direct modulation. IM/DD method can be employed for transmitting either single modulated RF signal or sub-carrier multiplex (SCM) modulated RF signals. At the receiver side these RF signals can be simply retrieved by detecting the optical carrier using a photo-diode, as shown in Figure 3.8.

3.2.2 Remote Heterodyne Detection (RHD) Method

The RHD method can be done by coherently mixing the two optical carriers at the PD that results in a high-frequency current I_{RF} at the output of the PD, as discussed in Equation 3.3 [37].

Optical generation of mm-wave signals can be done by beating two optical carriers at a photo-detector (PD), as shown in Figure 3.9. Let we have two optical carriers given by

$$E_1(t) = E_{01}\cos(\omega_1 t + \phi_1) \tag{3.1}$$

and

$$E_2(t) = E_{02}\cos(\omega_2 t + \phi_2) \tag{3.2}$$

Where E_{01} and E_{02} are the amplitude values of the optical waves $E_1(t)$ and $E_2(t)$, respectively. While ϕ_1 and ϕ_2 are the phase values of the optical waves

$E_1(t)$ and $E_2(t)$, respectively. The current at the output of the PD can be written as [38]:

$$I_{RF} = 2R\sqrt{P_1 P_2}\cos[(\omega_1 - \omega_2) + (\phi_1 - \phi_2)] \tag{3.3}$$

Where R is the responsivity of the PD and P_1 and P_2 are the optical power terms of two optical waves, respectively. As shown in Figure 3.9, the generation of mm-wave signals at a PD can be done by beating two optical carriers of two different LDs together. It is important to note that both the optical carriers at the input of PD are uncorrelated in frequency and phase. 3-dB optical coupler is used to multiplex both optical carriers. This technique is widely employed in the optical communication systems for the generation of mm-wave signals. But the disadvantage of using uncorrelated LDs is that their is a chance of frequency and phase instability [39].

We will discuss in the next section that how one can optically generate high frequency signals at the output of PD by using a single laser diode with the help of OCS technique, as shown in Figure 3.10.

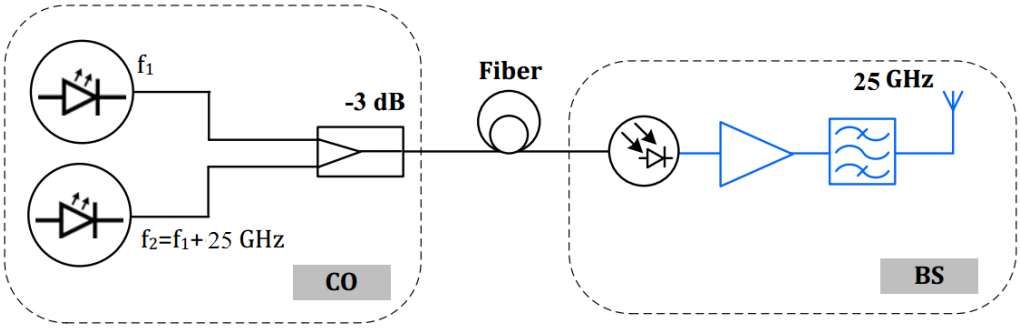

Figure 3.9: Schematic diagram of remote heterodyne detection for optically generated mm-wave RF signals at PD by using two laser diodes

3.2.3 Optical Carrier Suppression (OCS) Method

An attractive method for the generation of high frequency RF signals has been proposed in [40]. In the proposed method, instead of using simple IM/DD technique or two LDs to achieve mm-wave signal at the output of PD it biased the DD-MZM at the minimum transmission point. Because of the biasing at the minimum transmission point, the optical carrier is suppressed and the frequency of the optically generated radio signal at the BS is twice the RF signal originally fed to the DD-MZM at CO, as shown in

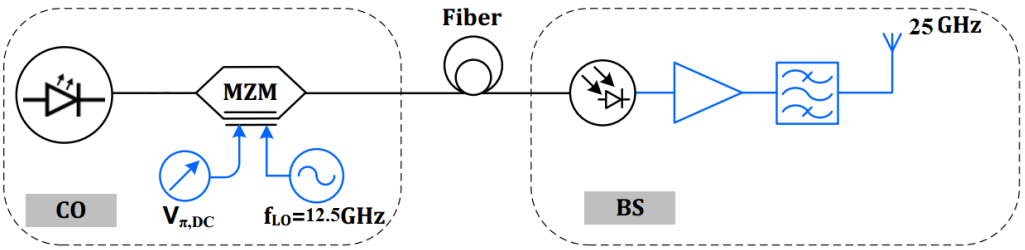

Figure 3.10: Schematic diagram for optical carrier suppression method

Figure 3.10.

In our proposed architecture, we achieved the **frequency doubling** of the modulating frequency f_{LO} signal by biasing the dual-drive MZM (DD-MZM) at the minimum transmission point [41], as shown in Figure 3.10.

Figure 3.11 shows the different biasing points at which MZM can be operated, that include Peak point (PP) biasing, Quadrature point (QP) biasing and Null point (NP) biasing.

- For **NP** biasing, the bias voltage $V_{bias} = (V_{DC1} - V_{DC2})$ should be configure to V_π.
- For **PP** biasing, the bias voltage $V_{bias} = (V_{DC1} - V_{DC2})$ should be configure to 0.
- For **QP** biasing, the bias voltage $V_{bias} = (V_{DC1} - V_{DC2})$ should be configure to $0.5 \times V_\pi$

To achieve Optical carrier suppression (OCS) at the output of DD-MZM, the bias voltage V_{bias} is applied at Null biasing point. When the modulating voltage of $V(t) = V_{RF}\cos(\omega_{RF}t)$ is applied to the DD-MZM then the mathematical expression for the photo detected RF signal in the case of NP biasing operation obtained from 2.6 can be written as:

$$I_{NP}(t) \propto P_{NP}(t) \tag{3.4}$$

$$P_{NP}(t) \quad = P_{in}\left[1-\cos\left(\frac{\pi V_{LO}\cos(\omega_{LO}t)}{V_\pi}\right)\right] \tag{3.5}$$

$$P_{NP}(t) = P_{in}\left[1-J_0\left(\frac{\pi V_{LO}}{V_\pi}\right)-2\sum_{n=1}^{\infty}(-1)^n J_{2n}\left(\frac{\pi V_{LO}}{V_\pi}\right)\cos(2n\omega_{LO}t)\right] \tag{3.6}$$

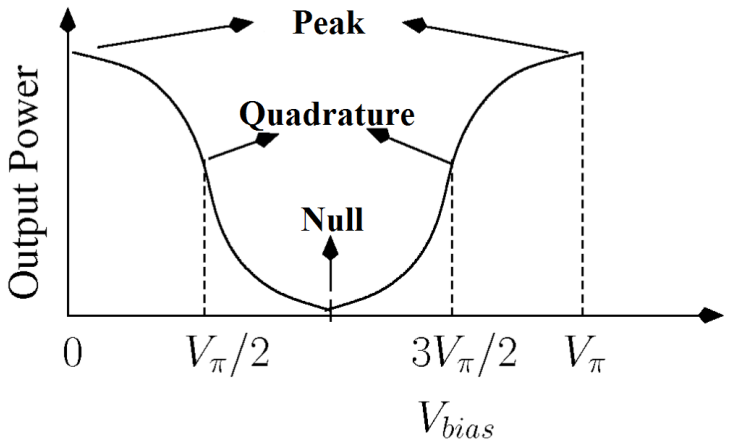

Figure 3.11: Biasing points for Mach Zehnder Modulator (MZM)

3.3 Method of Generating Multiple Optical Carriers using Optical Fiber

Wave-mixing is a phenomenon in which two or more optical carriers of different wavelengths non-linearly interact with each other to produce an idler wave at a new frequency. Four-wave mixing (FWM) is a process in which three (or two) waves are injected into a third order non-linear material to generate a an idler signal at new frequency. According to the number of injected optical wave into non-linear material, FWM process can be further divided into following two types:

- Non-Degenerate Four-Wave Mixing (FWM)
- Degenerate Four-Wave Mixing (FWM)

In ***non-Degenerate FWM*** process, three high power optical waves $E_1(t)$, $E_2(t)$ and $E_3(t)$ are injected into the Dispersion-shifted Fiber (DSF). These optical waves have angular frequency and phase of ω_1, ω_2, ω_3, φ_1, φ_2 and φ_3, respectively. Under the phase-matching condition, these optical waves non-linearly interact with each other and as a result forth wave is generated, the resultant polarization vector field can be described as [42]:

$$P(t) \propto \chi^3 \left[E_1(t) + E_2(t) + E_3(t)\right]^3 \tag{3.7}$$

As shown in Figure 3.12, because of the interaction of three waves, multiple idler signals are generated at angular frequencies:

$$\omega_{FWM1} = \omega_1 + \omega_2 - \omega_3, \tag{3.8}$$

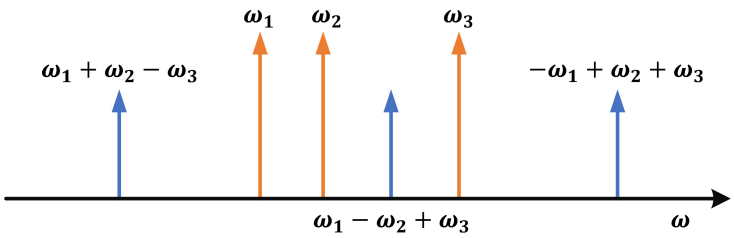

Figure 3.12: Non-Degenerate Four-Wave Mixing (FWM) Process

$$\omega_{FWM2} = \omega_1 - \omega_2 + \omega_3, \tag{3.9}$$

$$\omega_{FWM3} = -\omega_1 + \omega_2 + \omega_3, \tag{3.10}$$

The Phenomenon of FWM can also be occurred in DSF with two injected optical signals $E_1(t)$ and $E_2(t)$, with respective phase and angular frequency of φ_1, φ_2, ω_1 and ω_2 and hence it is also known as ***degenerate FWM*** [43]. Under the phase-matching condition, the resultant polarization field can be written as [42]:

$$P(t) \propto \chi^3 \left[E_1(t) + E_2(t)\right]^3 \tag{3.11}$$

As shown in Figure 3.13, the idler signals are generated at frequencies:

$$\omega_{FWM1} = 2\omega_1 - \omega_2, \tag{3.12}$$

$$\omega_{FWM2} = 2\omega_2 - \omega_1, \tag{3.13}$$

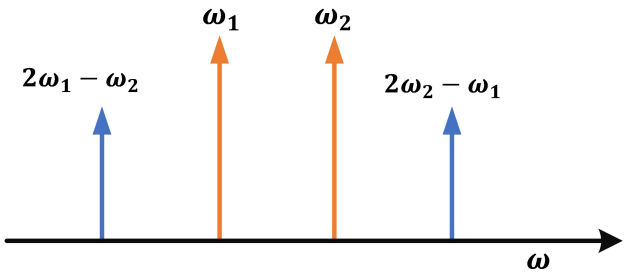

Figure 3.13: Degenerate Four-Wave Mixing (FWM) Process

3.4 Type of Noises in mm-wave RoF links

There are multiple types of noises in the RoF links which includes amplified spontaneous emission (ASE) noise at the EDFA amplifier, relative intensity noise (RIN) at the LD, shot noise and receiver's thermal (johnson) noise. At the receiver, δf is the bandwidth over which power of noise is calculated [3]. At the output of the LD there are certain variations in the output intensity, phase and frequency which contribute the above described **RIN**. Main reason of RIN is the spontaneous emission of photons, in which the intensity noise contributes the degradation in SNR while the frequency/phase noise is responsible for non-zero spectral beamwidth of the output frequency [3]. Mathematically, RIN noise can be written as:

$$\sigma^2_{RIN} = K_{RIN} I^2_{dc} \Delta f, \tag{3.14}$$

Where I_{dc} is the average current term, K_{RIN} is the device dependent term and usually its value is around $-150 dB/Hz$. **ASE** noise is due to the spontaneous emission of photons in the EDFA amplifiers that is further amplified because of the EDFA's gain mechanism.

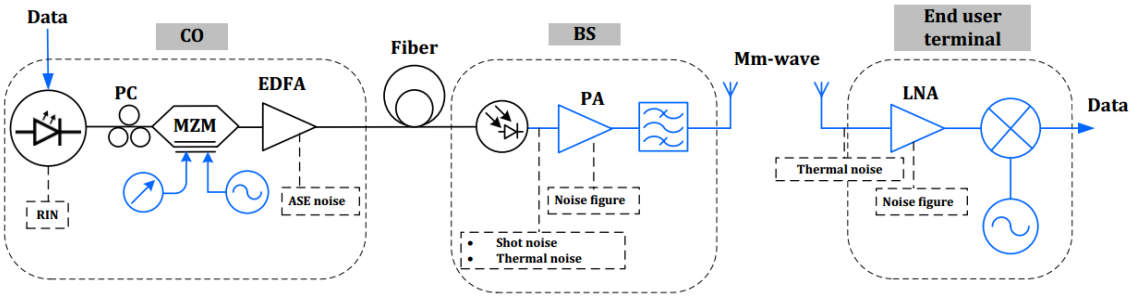

Figure 3.14: Noise contributions in RoF communication links

Shot Noise is a quantum noise phenomenon which is included in the output received electrical signal. This type of noise increases because of the reason that electric current and optical field comprises of different entities such as electrons and photons, respectively. It can be mathematically represented as [3]:

$$\sigma^2_{shot} = 2eI_{dc}\Delta f \tag{3.15}$$

Here the charge on an electron is denoted by e.

Finally, **Thermal Noise** is due to the load resistors and electrical amplifiers at the receiver side. It can be mathematically represented as [3]:

$$\sigma^2_{thermal} = \frac{4k_bT}{R_L}\Delta f \tag{3.16}$$

Here R_L is the load resistor term, T is the absolute temperature term and k_b is the Blotzmann constant. Thermal noise is also known as the johnson's noise and it is because of the temperature dependent random Brownian motion of electrons.

Chapter 4

Literature Review

4.1 Radio over Fiber Cost Reduction Methods

In this section the different kinds of cost reduction techniques especially proposed for the ROF communication systems are discussed. The set of methods designed for implementing wavelength reuse in the uplink and the set of methods used for the reduction in the number of laser diodes are discussed in section 4.1.1 and 4.1.2, respectively.

4.1.1 Wavelength Reuse Techniques

It is an optical duplexing method in which the uplink data transmission is done by reusing the optical signal of DL at the RAU. A significant cost reduction is achieved by using this technique, because for the uplink communication there is no need to have the optical sources at the RAUs, when this technique is employed. But by sharing the a portion of optical power of downlink to the uplink communication causes the performance degradation for downlink. In the past different methods for achieving the wavelength reuse such as optical re-modulation (ORM), optical carrier recovery (OCR) and reuse and modulator-cum photodetector are employed. A list of influential papers related to wavelength reuse methods are discussed in Table 4.1.

4.1.2 Reducing the Number of Laser Diodes

A multi-mode laser is capable of generating multiple tones at different frequencies of separation $\Delta\omega$. [58] and [59] employed multi-mode laser to support multiple RAUs, as discussed in Table 4.2.

[61] and [35] employed a single pulsed laser source to support multiple RAUs in a DAS architecture. While [56], [28] and [57] employed the modulation harmonics of DD-MZM to support multiple harmonics, as discussed in Table 4.2.

In Section 4.1.1, the techniques are discussed to make the RAUs laser free but in this section the family of techniques are discussed which helps to reduce the number of laser diodes at the CU.

Although the wavelength reuse techniques make the RAUs laser free but still a number of laser sources are required at the CU to support multiple RAUs. A lot of research work is done to reduce the number of optical sources at the CU and to increase the coverage with the minimum number of laser sources at the CU.

Table 4.1: Wavelength Re-use techniques for the cost-effective Radio over Fiber Systems

Authors	Contribution
Welstand et al. 1996 [44]	Introduced the concept of simplex operation of EAM by switching the bias voltage of EAM as modulator-cum photo-detector
Noel et al. 1997 [45]	Introduced the concept of bidirectional operation of EAM of single bias voltage as modulator-cum photodetector at the cost of performance trade-off between DL and UL
Wu et al. 1998 [46]	Introduced the idea of reusing the optical carrier by for uplink wireless signal transmission by proposing the the optical re-modulation (ORM) method
Stohr et al. 1999 [47]	To implement the technique of wavelength reuse, two lasers were used to implement the operation of EAM as modulator-cum photodetcetor
Nirmalathas et al. 2001 [48]	Introduced the concept of Optical Carrier Recovery and Reuse (OCRR) in the Radio Access Point (RAP) using Fiber Bragg Grating (FBG) and optical coupler
Bakaul et al. 2005 [49]	Introduced the concept of Optical Carrier Recovery and Reuse (OCRR) in the Radio Access Point (RAP) of a ROF systems by employing Wavelength-Interleaved WDM (WI-WDM) signals
Jia et al. 2006 [50]	Implemented the OCRR technique to generate the frequency doubled RF signals by using optical circulator and FBG
Yu et al. 2007 [51]	Implemented the Optical Carrier Recovery and Reuse (OCRR) technique along with the DL frequency doubling by employing an interleaver
Won et al. 2007 [52]	Implemented optical re-modulation (ORM) method by employing a Reflective Semiconductor Optical Amplifier (RSOA)
Olmos et al. 2007 [53]	Proposed the reconfigurable RoF architecture by using the multi-mode laser diode
Haung et al. 2008 [54]	Downlink frequency quadrupling was used along with the OCRR technique to achieve wavelength reuse
Ji et al. 2009 [55]	ORM architecture was implemented by employing optical phase modulator in the DL and optical intensity modulator in the UL, respectively
Chowdhury et al. 2009 [56]	Implemented the multi-band transmission of WiFi WiMax and mm-wave RF signals by employing the multiple harmonics generated by optical modulation
Thomas et al. 2013 [57]	By employing DD-MZM, optical carrier generation was achieved at the CU to improve the performance of UL data transmission

Table 4.2: Family of ROF cost reduction techniques by reducing the number of optical sources at the CU

Authors	**Contrinutions**
Kuri et al. 2005 [58]	Multi-mode laser was used to generate up to 360 channels which can support ROF bidirectional communication with 180 RAUs
Nakasyotani et al. 2006 [59]	Multi-mode laser was used along with SCM technique to support up to 10080 RF channels of 60 GHz frequency in WDM ROF communication
Chowdhury et al. 2009 [56]	It used modulation harmonics produced by the external phase modulator to support the transmission of WiMAX, WiFi and 60 GHz RF signals to a RAU
Hsueh et al. 2009 [60]	It experimentally demonstrated the feasibility of transmitting multi-band DL RF signal including mm-wave, microwave and base-band signals by using a single CW laser and an intensity modulator
Ghafoor et al. 2011 [28]	It employed modulation harmonics generated by DD-MZM to support two RAUs in a DAS architecture
Ghafoor et al. 2012 [61]	It employed a single pulsed laser source and a single optical fiber to support duplex DROF architecture
Thomas et al. 2013 [57]	It employed modulation harmonics generated by a single optical modulator to support duplex diversity assisted AROF in the DL and DROF in the UL. Single laser source is used at CU to support four RAUs in a ring architecture
Thomas et al. 2013 [35]	It employed a pulsed semi-conductor laser to support six RAUs in simplex BROF star-like DAS architecture
Tang et al. 2016 [62]	A single LD is used at CU to experimentally demonstrate the feasibility of bidirectional ROF link for short range applications is which is based on a dual-polarization MachZehnder modulator (DPol-MZM)

Chapter 5

Optical Signal Processing Based RoF architecture

5.1 Coordinated Multipoint (CoMP) Architecture

Coordinated multi-point (CoMP) system is a radio access architecture which exploits all the available antenna terminals at RAUs by employing joint processing (JP) schemes in both DL and UL. The capacity of the CoMP system can be measured as the capacity of the corresponding multiuser virtual MIMO channels, where all the antenna terminals of all RAUs are pooled to jointly transmit and receive mm-wave signals to and from the mobile users (MS).

The gain proposed by the COMP architectures comes from the fact that as the number of antenna terminals connected with the CU increases, the rate of multiple access channels and broad-casting rises linearly too. The key factors for these gains are the JP techniques which are used in the CoMP system. These JP techniques can be employed with a centralized or distributed DAS architecture [26].

The centralized DAS architecture relies on a CU which is connected to multiple low-cost RAUs and CU is responsible for executing all the joint processing CoMP (JP-CoMP) algorithms. The transmission between CU and RAUs can be either analog or digital.

In Digital-ROF (**DROF**) links, the digital samples are transmitted from the CU to (or from) the RAUs by using optical fiber links. The digital-to-

analog conversion (D/A), analog-to-digital conversion (A/D), down-conversion and up-conversion is required at each RAU to transmit (or receive) high frequency RF signals to the MS.

On the other hand, in analog-ROF (**AROF**) links, the RF signals are transmitted from the CU to (or from) the RAUs by using optical fiber links. Unlike the DROF links, the baseband signals generation is done at the CU and not in the RAUs. In AROF system, the complexity is shifted from the RAUs to the CU as compared to the DROF system (e.g. no A/D and D/A conversion is required at the RAUs).

In our thesis, we assume a centralized DAS architecture where K RAUs are connected with a single CU via AROF link, as shown in Figure 5.1. Each RAU has the same number of L antenna terminals and M mobile users are placed randomly in the area of interest. DPSK modulation is used for both UL and DL. The channel matrix between RAU $k\,\varepsilon(1....K)$ and user $m\varepsilon(1....M)$ is represented by $\mathbf{H}_{m;k}$ for the UL and $\tilde{\mathbf{H}}_{m;k}$ for the DL. Similarly, the channel matrix between m user and all the RAUs is represented by $\mathbf{H}_m$ for the UL and $\tilde{\mathbf{H}}_m$ for the DL.

In the uplink, we assumed that all the data signals received from K users are decoded by the CoMP algorithms at CU by processing the received signals from all L antenna terminals deployed at all K RAUs.Where as in the downlink, it is assumed that CoMP system exploits L antenna terminals deployed at K RAUs to transfer symbols to the users.

5.2 The Proposed ROF Architecture

5.2.1 Introduction

In this section, the novel contributions towards the physical layer design of proposed centralized DAS architecture is discussed. the throughput per mobile user can be increased in a centralized DAS architecture by using the high frequency mm-wave signals. As the frequency increases the path-loss increases too, hence small cells are required because of the reduced propagation range of mm-waves [63]. As the size of the cell decreases due to the reduced propagation range of mm-waves, the number of cells increases to cover a large geographical area. In order to propose cost-efficient ROF architecture for operating companies, the RAUs must be simple and low-cost [64]. Because of the low-attenuation, high bandwidth, and transparency to mm-wave signals, the optical fiber plays a vital role to connect RAUs with the

cental unit (CU). As shown in Figure 5.1, all the RAUs are connected with the CU through optical fiber, all the resource management and joint signal processing tasks of RAUs can be effectively done at a single CU in centralized CoMP infrastructure [33].

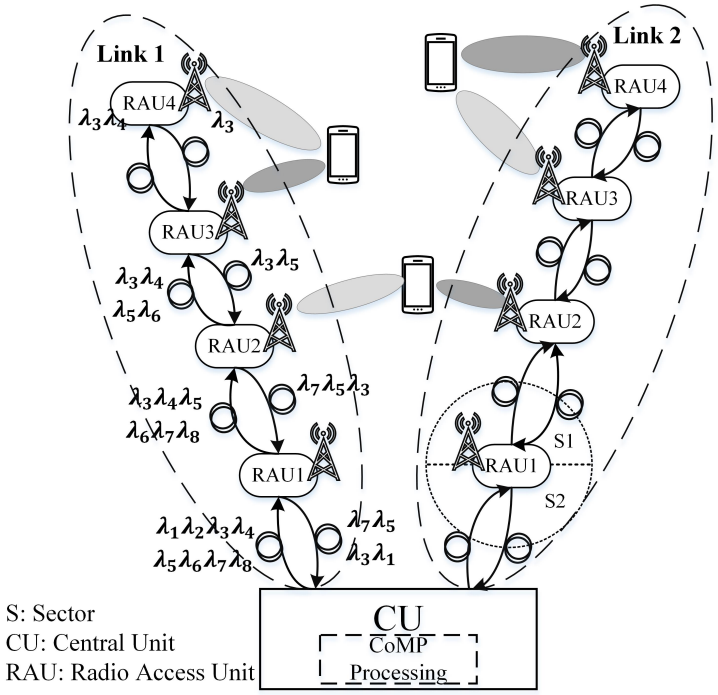

Figure 5.1: Proposed coordinated multi-point (CoMP) architecture

CoMP architecture is shown in Figure 5.1, where all the RAUs are assumed as the elements of DAS. Let Link 1 of the architecture, which compraises of four RAUs connected to the CU through two spans of Optical fiber. As discussed in Section 5.1, mobile users (MU) are distributed randomly in the area of interest and each RAU is surrounded by multiple MSs. Depends upon the received signal strength, each MS can be wirelessly connected to multiple antenna terminals of different RAUs by employing CoMP based algorithms. CU may be connected to multiple links in a star-like architecture but to avoid the complexity of the system we only discuss two links, as shown in Figure 5.1. The main goal of the 5G wireless networks is to increase the capacity per user by exploiting the gain achieved by the CoMP algorithms employed by centralized DAS architecture. In order to transfer mm-wave frequencies, the dispersion-induced fiber impairments linked with high data rate optical carriers must be quantified.

As briefly discussed in Table 4.1 and in Table 4.2, in order to get cost-

effective ROF systems a huge amount of research has been conducted in the past to eliminate the need of laser source at RAUs for uplink communication as well as to reduce the number of laser sources used at CU. In the recent years a considerable amount of research is also done to generate mm-wave signals at CU using low-frequency Local Oscillators (LO). Usually RHD techniques are used at the RAUs to generate mm-wave RF signals as shown in Figure 3.9, where two laser diodes are used to achieve mm-wave RF signals at the output of PD. However, the use of two laser sources to get RHD requires complex signal processing to get coherent optical carriers at the input of PD. To generate multiple phase-coherent optical carriers from a single laser source, OCS technique of Section 3.2.3 is proposed in [41] to generate three reduced-rate RF signals at a single RAU [41] in a ring architecture.

Similarly, in [28] single laser source along with the OCS technique of Section 3.2.3 is utilized to generate multiple phase-coherent side-bands to transmit (and receive) 4 SCM signals to (and from) two RAUs in a duplex manner. Additionally, a single low frequency LO of 12.5 GHz is used at CU to generate 25 GHz four mm-wave signals at both RAUs. But in the uplink, 4 SCM base-band signals are transmitted from both RAUs to the CU. In [57] a single laser source along with the OCS technique is used to support four RAUs in a ring architecture but the use of optical add and drop multiplexer (OADM) at each RAU makes this architecture less attractive.

Against this background, the novel contributions of this paper are:

1. The generation of multiple optical carriers using a single laser source is done by using OCS technique and optical frequency comb (OFC) generator in DD-MZM and optical fiber medium, respectively.

2. The feasibility of transmitting two sub-carrier multiplexed (SCM) 256 Mbps DPSK mm-wave signals from CU to four RAUs and receiving 128 Mbps DPSK mm-wave signals from four RAUs is done by using coherent optical carriers for achieving RHD.

3. The propose scheme is capable of simultaneously transferring ROF signals to 4 RAUs in a duplex architecture by using a a single laser diode located at CU.

The basic idea behind the centralized DAS architecture is to move the remote antennas of a virtual MIMO (CoMP) system closer to the cell-edge in order to reduce the path loss, to provide uniform radio coverage with better signal strength and hence improves the cell-edge throughput. In the CoMP infrastructure the antenna terminals deployed in each RAU are connected

to a single CU through optical fiber. We designed and simulated a novel cost-effective solution for CoMP system application which imposes a lot of design challenges.

5.2.2 Physical Layer Architecture

Figure 5.2 shows the physical layer architecture of link 1 of DAS architecture, as shown in Figure 5.1. Eight coherent optical carriers are generated from a single laser diode by employing OCS and OFC generation techniques, as discussed in Section 3.2.3 and in Section 3.3, respectively. The low frequency LO is applied to the DD-MZM of Section 2.1.2 for the purpose of generating required optical side-bands with the frequency spacing of 25 GHz. To achieve OCS, the operating DC bias of amplitude $0.7V_\pi$ is applied at the Null biasing point of DD-MZM, as shown in Figure 3.11. Where V_π is the voltage required to induce the phase-shift of π in each arm of DD-MZM. The first-order odd indexed side bands of frequency 193.1125 GHz and 193.0875 GHz are obtained during OCS while the optical carrier and the even-indexed sidebands are highly attenuated during OCS process, as seen in the optical spectrum of Figure 5.3. To remove unwanted frequencies other then first-order odd indexed optical carriers with the spacing 25 GHz, the output of DD-MZM is optically splitted using 3-dB (1×2) optical splitter (OS) and fed to the Gaussian optical bandpass filters (OBPF) with a 3-dB bandwidth of 15 GHz centered at 193.1125 GHz and 193.0875 GHz, respectively. The outputs of the OBPFs are coupled using optical coupler (OC) and amplified using Erbium dopped fiber amplifier (EDFA) of noise-figure 6 dB.

The amplified signals are injected into the highly nonlinear dispersion-shifted fiber (HNL-DSF) to get OFC by utilizing the phenomenon of Degenerate FWM of Section 3.3. Due to the imperfection of OCS and OFC generation technique, the even indexed side-bands are still present in the spectral plot of Figure 5.4. Third-order non-linear optical fiber of length 0.5 Km generates eight optical carriers, as shown in the optical spectrum of Figure 5.4. To get eight discrete optical carriers, the output of the HNL-DSF is fed to the (1×8) AWG of spacing 25 GHz which performs 3-dB Gaussian filtering of bandwidth 25 GHz. The optical carriers obtained at the output of AWG are denoted as λ_1, λ_2, λ_3, λ_4, λ_5, λ_6, λ_7 and λ_8, as shown in Figure 5.2.

The optical carrier named as λ_1, λ_3, λ_5 and λ_7 are intensity modulated using single-drive MZM with two SCM DPSK RF signals for the DL data transmission. Each RF signal has a data-rate of 256 Mbps and the SCM

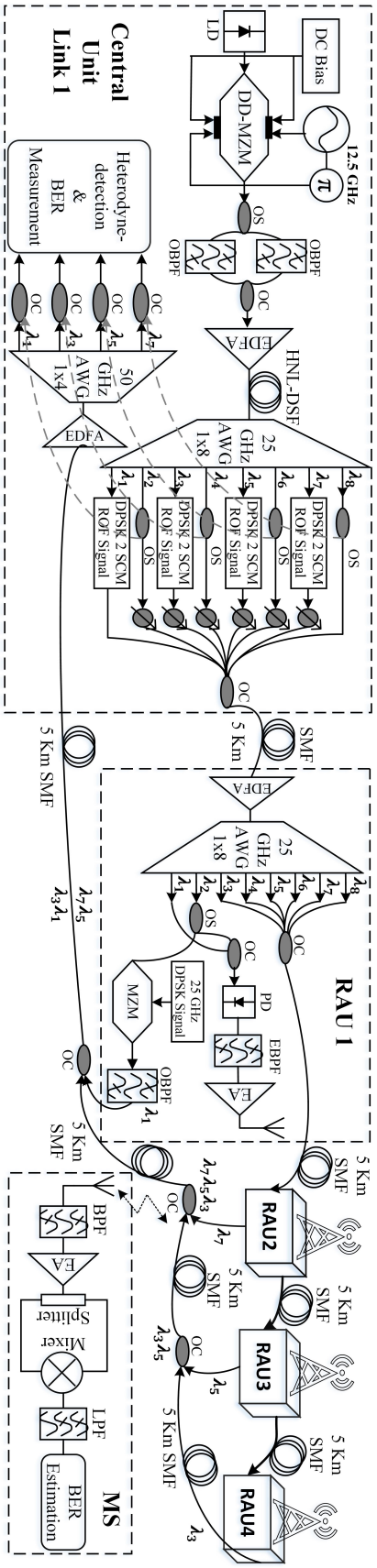

Figure 5.2: Physical layer architecture of mm-wave carrying centralized DAS

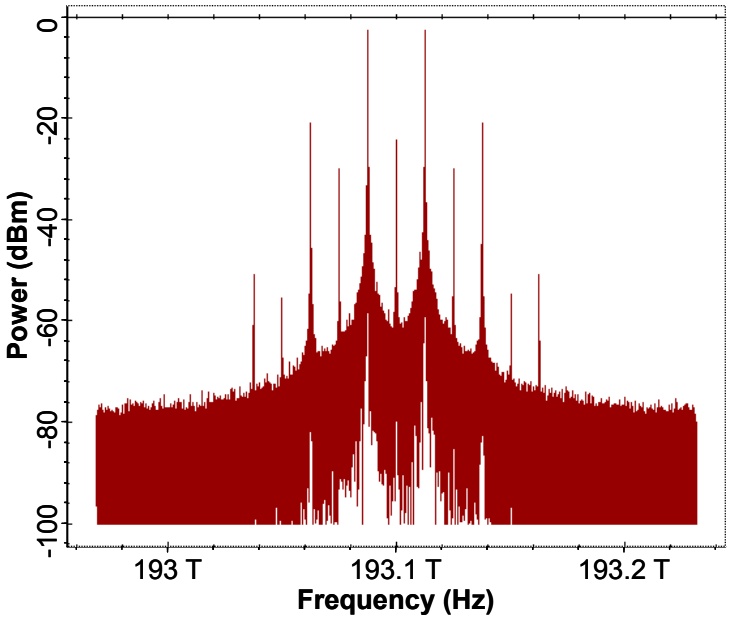

Figure 5.3: Spectral plot at the output of Dual-drive MZM

signal $X_m(t) = f_1(t) + F_2$ obtained has the frequencies $f_1(t) = 500$ MHz and $f_1(t) = 1$ GHz. Hence the total data rate delivered to each RAU is 512 Mbps (2 channels x 256 Mbps).

To avoid the effect of XPM specially on the modulated optical carriers, the optical carriers λ_2,...., λ_7 are attenuated by using optical attenuators (OA). While travelling in the SMF, the phase noise imposed by the XPM is converted into the amplitude noise due to the mechanism of fiber induced dispersion. As the power of the optical carrier increases the phase noise increases too and hence the average power per carrier should be kept low. After attenuating the optical carriers, all the modulated and un-modulated carriers are coupled together using OC and the spectral plot of the composite signal is shown in Figure 5.5.

The composite signal is traveled from the central unit to the RAU1 via 5 Km SMF, as shown in Figure 5.2. At the RAU1 the received composite signal is amplified and fed to the 25 GHz (1×8) AWG for the purpose of de-multiplexing. The EDFA is attached before the AWG so that the generated ASE noise by the amplifier can be filtered by AWG. λ_2 is splitted into two parts where one part is used for the intensity modulation of the 25 GHz uplink DPSK RF signal using single-drive MZM. While the second part is

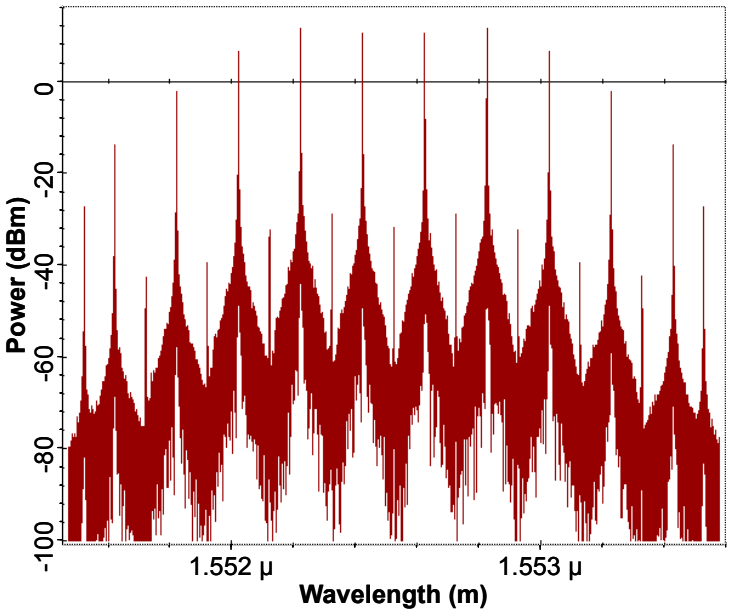

Figure 5.4: Spectral plot at the output of HNL-DSF

coupled with modulated carrier λ_1 by using OC to generate 25 GHz mm-wave signal by utilizing RHD at PD as discussed in Section 3.2.2. The PD has the dark current of 2 nA, responsivity of 0.9 A/W and a thermal noise of value $10 \times 10^{-12}\ A/\sqrt{W}$. After the PD the unwanted frequencies generated during the process of photo-mixing are removed from the desired signal by using a 3 dB electric bandpass filer of central frequency 25 GHz and having a bandwidth of 5 GHz. At that point the mm-wave signal can be directly transmitted from the antenna terminal of RAU1 to the MU through wireless medium but in order to measure the quality of the received signal, the mm-wave is down converted to the baseband frequency by using the process of self-mixing, as shown in Figure 5.2. First-order modulated side-band λ_1 generated during the intensity modulation of λ_2 by 25 GHz RF signal is filtered using Gaussian OBPF having a central frequency of $(\lambda_1 = \lambda_2 - 25GHz)$. The resultant single sideband (SSB) optical carrier is sent towards the CU for processing, as shown in Figure 5.2. At RAU1,the discrete optical carriers λ_3, λ_4, λ_5, λ_6, λ_7 and λ_8 are optically coupled using OC and transmitted to the RAU2 through 5 Km SMF.

At RAU2, the composite signal is amplified and fed to the 25 GHz (1×6) AWG for Gaussian filtering the carriers. The power of Optical carrier λ_8 is divided into two parts using 3 dB 1×2 OS, where upper part is coupled

with the modulated carrier λ_7 using OC and fed to the PD for the purpose of generating mm-wave RF signal. While the lower part of λ_8 is used to intensity modulate the 25 GHz uplink data received from the MU. The output of the single-drive MZM is fed to the OBPF having a central frequency of λ_7 in order to remove the unwanted frequencies from the spectrum and the resultant modulated SSB signal λ_7 is transmitted towards the CU for JP. At RAU2, the optical carriers named as λ_3, λ_4, λ_5 and λ_6 are coupled together using OC and transmitted towards the RAU3 via 5 Km SMF.

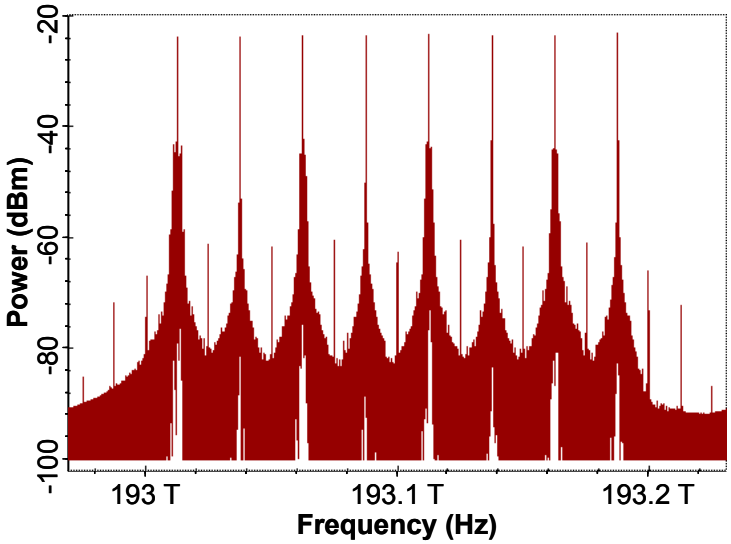

Figure 5.5: Spectral plot of the combined optical signal before transmitting from towards RAU1

Similarly, at RAU3 before injecting the composite signal into the 25 GHz (1×4) AWG for Gaussian filtering, the composite signal is amplified. Here unmodulated optical carrier λ_6 is splitted using OS. The upper part of λ_6 is coupled with modulated carrier λ_5 to generate 25 GHz signal. While the lower part is intensity modulated with the 25 GHz UL data signal by using single-drive MZM. $(\lambda_5 = \lambda_6 - 25GHz)$ is Gaussian filtered using OBPF in order to remove the unwanted frequencies. Optical carriers named as λ_3 and λ_4 are coupled using OC and transmitted towards RAU4 through 5 Km SMF.

At RAU4, the amplified composite signal is Gaussian filtered using 25 GHz 1×2 AWG. The discrete unmodulated optical carrier λ_4 is splitted into two parts by employing OS. The upper part is coupled with the modulated carrier λ_3 and fed to the PD to get mm-wave RF signals at the output of the

photo-detector. While the lower part is used to carry 25 GHz UL RF data signal by using single-drive MZM. The left part of the first-order side-band is filtered using Gaussian OBPF of central frequency ($\lambda_3 = \lambda_4 - 25GHz$) and transmitted towards the RAU3 through 5 Km SMF for the purpose of JP at CU. At the RAU3, the UL data carrying signal λ_5 of RAU3 is coupled with the UL data carrying signal λ_3 of RAU4 by employing OC and the composite signal is transmitted towards RAU2 via 5 Km SMF. At the RAU2, the UL data carrying optical carrier λ_7 of RAU2 is coupled with the combined signal of λ_3 and λ_5 and the resultant signal is transmitted towards the RAU1 through 5 Km SMF. At RAU1, the composite signal of λ_3, λ_5 and λ_7 is coupled with the UL data carrying signal λ_1 of RAU1 and transmitted towards the CU through 5 Km SMF.
At CU, the combined signal first amplified using EDFA and then it is demultiplexed using 50 GHz 1×4 AWG. The received optical carriers λ_1, λ_3, λ_5 and λ_7 are respectively coupled with the optical carriers λ_2, λ_4, λ_6 and λ_8 to get mm-wave RF signals. DPSK demodulator is used for evaluating the BER values of all the mm-wave signals received at CU from each of the RAUs.

5.3 Performance of the Proposed DAS Architecture

Let us now discuss the BER results of out proposed architecture for the downlink and uplink signals of RAU1, RAU2, RAU3 and RAU4 in Figure 5.6 and Figure 5.7, respectively. The BER values are plotted against the optical received power of the modulated carriers. The optical attenuator (OA) is used to vary the power of the received signal. The variations in the BER results are done by varying the received signal power and the corresponding BER versus Optical received power (dBm) values are plotted in Figure 5.6 and Figure 5.7 for both DL and UL. As shown in Figure 5.5, the CU-RAUs downstream signal spectral plot comprises of eight optical sidebands. Four of these optical sidebands are intensity modulated using single-drive MZM to generate ODSB signals, while the optical carriers named λ_2, λ_4, λ_6 and λ_8 are transmitted without any modulation.

It can be seen from Figure 5.4, that the OSNR of the higher-order sidebands (third-order, fourth-order) is lesser compared to the first-order and second order side-bands. Because of the low OSNR of the high-order sidebands at the output of the HNL-DSF, higher ASE noise is generated at wavelengths named as λ_1, λ_2, λ_7 and λ_8. Hence, we use higher-order side-

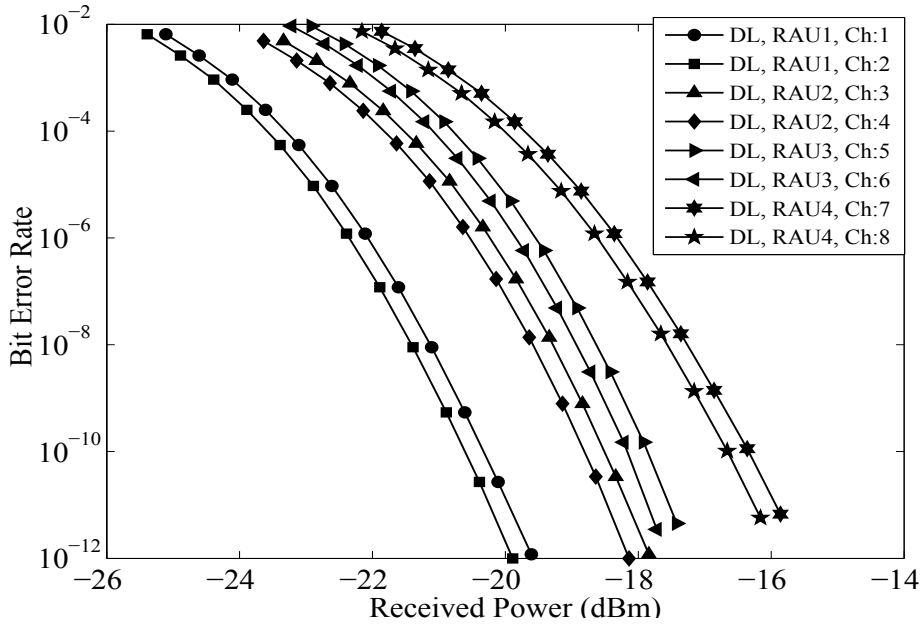

Figure 5.6: BER versus received optical power (dBm) plot for downstream RF signals

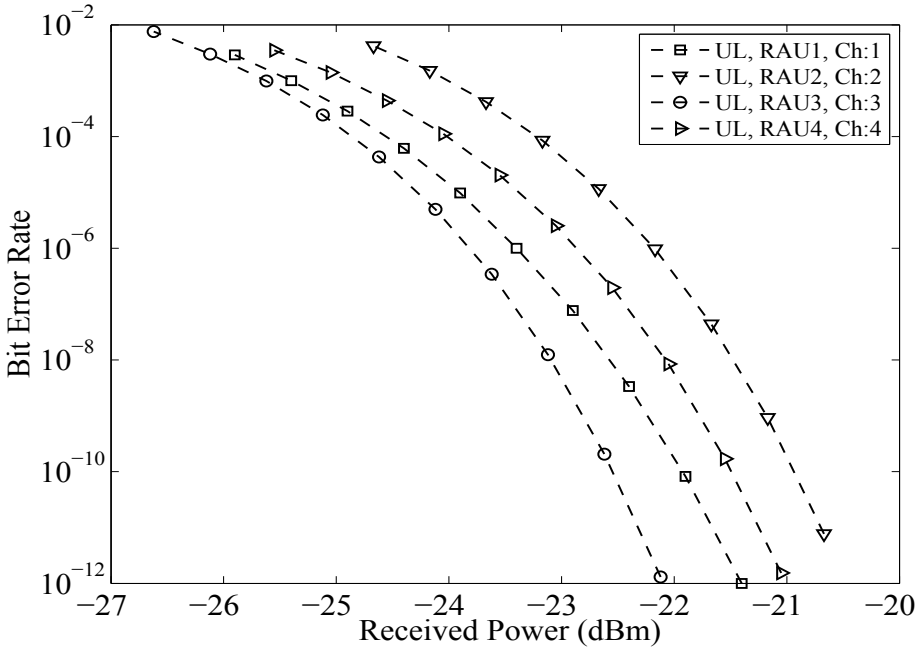

Figure 5.7: BER versus received optical power (dBm) plot for upstream RF signals

bands for relatively closer RAUs. For instance, signals λ_1, λ_2 are used for the transmission and reception of mm-wave signals from 5 Km away RAU1, while λ_7 and λ_8 are used for the transmission and reception of mm-wave signals from 10 Km away RAU2. Similarly, lower-order (first-order, second-order) side-bands with higher OSNR compared to higher-order sidebands are used for RAU3 and RAU4 which are 15 Km and 20 Km away from the CU, respectively. for example, signals λ_5 and λ_6 are responsible for transmitting and receiving mm-wave signals from 15 Km away RAU3, while signals λ_3 and λ_4 are used at RAU4 which is 20 away from the CU. It may be seen from Figure 5.6, apart from the OSNR difference between the high-order sidebands and low-order sidebands, the receiver sensitivity also depends upon the length of the fiber. It may be observed from Figure 5.6 that as the length of the SMF increases the value of the receiver sensitivity also increases. For instance, in the DL the value of maximum receiver sensitivity is obtained from the channel 7 and channel 8 which is around -17 dBm, while the minimum value receiver sensitivity is obtained form the channel 1 and channel 2 which is around -21.25 dBm. Similarly, in the UL the maximum value of receiver sensitivity is obtained form channel 2 which is around -21.40 dBm, while the minimum value is for channel 3 which is around -23 dBm. As discussed earlier, the reason behind the variation in receiver sensitivities is due difference between the OSNR of higher-order and lower-order sidebands. Overall, Acceptable BER values are obtained for bothuplink and downlink mm-wave signals by employing different components having the parameter values similar to the characteristics of the commercially available components used RoF communication systems.

Chapter 6

Conclusion and Future Work

6.1 Conclusion

RoF systems are expected to build the backbone of future 5G wireless networks. In RoF architecture, the installation cost of the optical infrastructure and the achievable link performance are the key matrices. In this thesis we have proposed the centralized DAS architecture which is responsible for feeding four RAUs by employing a single LD. In the DAS architecture, processing of all RAUs is jointly done at CU by using CoMP algorithms. The proposed DAS used AROF links to transmit 2-SCM, DPSK RF signals to four RAUs which are located at 5 Km, 10 Km, 15 Km and 20 Km from the CU in a CoMP architecture. In the downlink, 512 Mbps 2-SCM mm-wave signals are transmitted to each RAU from the CU while 128 Mbps mm-wave signals are transmitted from each RAU to the CU. A single laser source and low-frequency LO is used to transmit and receive data carrying mm-wave signals to (and from) the RAUs. The DAS architecture is characterized by observing the BER results of Figure 5.6 and Figure 5.7 for both downlink and uplink signals by employing the optical components having the parameter values almost similar to the practical components available in the market.

6.2 Future Directions

6.2.1 Optical Wireless Communication based Data-Centers (DCs)

Currently, most of the installed DC networks (DCNs) employed wired connections such as optical fiber or copper cables for the purpose of inter-rack or intra-rack communication. Because of the disadvantages of hotspot and cabling complexity, the network research community propose the use of optical wireless communication or free-space optics (FSO) technology in DCNs. Most commonly used light source in the FSO links are highly directional Laser Diodes (LDs) which can support high data-rate transmissions. In the in-door FSO links, the atmospheric losses are negligible and because of this reason this technology is a strong wireless communication technology which can be used in future DCNs.

Therefore, our future work is to design and simulate cost-efficient FSO based duplex switch-centric wireless architecture, where optical wireless connection is established between the servers and the switching nodes. In switch-centric architecture, the servers of the DC are work as the computing nodes and the switches are responsible for the routing of the data.

Bibliography

[1] J. M. Senior and M. Y. Jamro, *Optical fiber communications: principles and practice*. Pearson Education, 2009.

[2] S. Ghafoor, *Radio over fiber systems*. PhD thesis, University of Southampton, 2012.

[3] G. P. Agrawal, "Fiber-optic communication systems,"

[4] G. Keiser, "Optical fiber communication," *NY: McGraw-Hill*, 2000.

[5] C. V. N. Index, "Global mobile data traffic forecast update, 2012–2017 http://www. cisco. com/en," *US/solutions/collateral/ns341/ns525/ns537/ns705/ns827/white paper c11-520862. html (Son erisim: 5 Mayıs 2013)*, 2013.

[6] A. Ericsson, "traffic and market data report–on the pulse of the networked society," 2011.

[7] v. d. D. D. Borne, *Robust optical transmission systems: modulation and equalization*. PhD thesis, Technische Universiteit Eindhoven, 2008.

[8] T. Berceli and P. R. Herczfeld, "Microwave photonics-a historical perspective," *IEEE transactions on microwave theory and techniques*, vol. 58, no. 11, pp. 2992–3000, 2010.

[9] M. Fice, E. Rouvalis, F. Van Dijk, A. Accard, F. Lelarge, C. Renaud, G. Carpintero, and A. Seeds, "146-ghz millimeter-wave radio-over-fiber photonic wireless transmission system," *Optics express*, vol. 20, no. 2, pp. 1769–1774, 2012.

[10] A. E. Siegman, "Lasers university science books," *Mill Valley, CA*, vol. 37, p. 208, 1986.

[11] G. Li and P. Yu, "Optical intensity modulators for digital and analog applications," *Journal of Lightwave Technology*, vol. 21, no. 9, p. 2010, 2003.

[12] X. Qian, P. Hartmann, J. D. Ingham, R. V. Penty, and I. H. White, "Directly-modulated photonic devices for microwave applications," in *Microwave Symposium Digest, 2005 IEEE MTT-S International*, pp. 4–pp, IEEE, 2005.

[13] W. Marshall, B. Crosignani, and A. Yariv, "Laser phase noise to intensity noise conversion by lowest-order group-velocity dispersion in optical fiber: exact theory," *Optics letters*, vol. 25, no. 3, pp. 165–167, 2000.

[14] K. Noguchi, O. Mitomi, and H. Miyazawa, "Millimeter-wave ti: Linbo3 optical modulators," *Journal of Lightwave Technology*, vol. 16, no. 4, p. 615, 1998.

[15] G. P. Agrawal, *Nonlinear fiber optics*. Academic press, 2007.

[16] S. Iezekiel, *Microwave photonics: Devices and applications*, vol. 3. John Wiley & Sons, 2009.

[17] G. H. Smith, D. Novak, and Z. Ahmed, "Overcoming chromatic-dispersion effects in fiber-wireless systems incorporating external modulators," *Microwave Theory and Techniques, IEEE Transactions on*, vol. 45, no. 8, pp. 1410–1415, 1997.

[18] R. Ramaswami, K. Sivarajan, and G. Sasaki, *Optical networks: a practical perspective*. Morgan Kaufmann, 2009.

[19] D. Marcuse, A. R. Chraplyvy, and R. Tkach, "Effect of fiber nonlinearity on long-distance transmission," *Lightwave Technology, Journal of*, vol. 9, no. 1, pp. 121–128, 1991.

[20] S. Kumar, *Impact of Nonlinearities on Fiber Optic Communications*, vol. 7. Springer Science & Business Media, 2011.

[21] B. C. Levy, *Principles of signal detection and parameter estimation*. Springer Science & Business Media, 2008.

[22] P. M. Becker, A. A. Olsson, and J. R. Simpson, *Erbium-doped fiber amplifiers: fundamentals and technology*. Academic press, 1999.

[23] C. R. Doerr and K. Okamoto, "Advances in silica planar lightwave circuits," *Journal of Lightwave Technology*, vol. 24, no. 12, pp. 4763–4789, 2006.

[24] H. Uetsuka, "Awg technologies for dense wdm applications," *Selected Topics in Quantum Electronics, IEEE Journal of*, vol. 10, no. 2, pp. 393–402, 2004.

[25] X. N. Fernando, *Radio over fiber for wireless communications: From fundamentals to advanced topics*. John Wiley & Sons, 2014.

[26] N. J. Gomes, P. P. Monteiro, and A. Gameiro, *Next generation wireless communications using radio over fiber*. John Wiley & Sons, 2012.

[27] J. Johny, *Radio over fiber-a new communication era: Future broadband wireless access*. LAP Lambert Academic Publishing, 2012.

[28] S. Ghafoor and L. Hanzo, "Sub-carrier-multiplexed duplex 64-qam radio-over-fiber transmission for distributed antennas," *Communications Letters, IEEE*, vol. 15, no. 12, pp. 1368–1371, 2011.

[29] S. Karabetsos, S. Mikroulis, and A. Nassiopoulos, "Radio over fiber for broadband communications: A promising technology for next generation networks," *Handbook of Research on Heterogeneous Next Generation Networking: Innovations and Platforms*, pp. 80–103, 2008.

[30] J. J. Vegas Olmos, T. Kuri, and K.-i. Kitayama, "Dynamic reconfigurable wdm 60-ghz millimeter-waveband radio-over-fiber access network: architectural considerations and experiment," *Journal of Lightwave Technology*, vol. 25, no. 11, pp. 3374–3380, 2007.

[31] H. Al-Raweshidy and S. Komaki, *Radio over fiber technologies for mobile communications networks*. Artech House, 2002.

[32] L. Hanzo, M. El-Hajjar, and O. Alamri, "Near-capacity wireless transceivers and cooperative communications in the mimo era: Evolution of standards, waveform design, and future perspectives," *Proceedings of the IEEE*, vol. 99, no. 8, pp. 1343–1385, 2011.

[33] L. L. Hanzo, O. Alamri, M. El-Hajjar, and N. Wu, *Near-Capacity Multi-Functional MIMO Systems: Sphere-Packing, Iterative Detection and Cooperation*, vol. 4. John Wiley & Sons, 2009.

[34] S. Betti, E. Bravi, and M. Giaconi, "Analysis of distortion effects in subcarrier-multiplexed (scm) externally modulated lightwave systems: a generalized approach," *Photonics Technology Letters, IEEE*, vol. 9, pp. 118–120, Jan 1997.

[35] V. A. Thomas, S. Ghafoor, M. El-Hajjar, and L. Hanzo, "Baseband radio over fiber aided millimeter-wave distributed antenna for optical/wireless integration," *Communications Letters, IEEE*, vol. 17, no. 5, pp. 1012–1015, 2013.

[36] A. Nirmalathas, P. A. Gamage, C. Lim, D. Novak, R. Waterhouse, and Y. Yang, "Digitized rf transmission over fiber," *Microwave Magazine, IEEE*, vol. 10, no. 4, pp. 75–81, 2009.

[37] U. Gliese, S. Norskov, and T. Nielsen, "Chromatic dispersion in fiber-optic microwave and millimeter-wave links," *IEEE Transactions on microwave theory and techniques*, vol. 44, no. 10, pp. 1716–1724, 1996.

[38] J. Yao *et al.*, "A tutorial on microwave photonics," *IEEE Photonics Soc. Newsl*, vol. 26, no. 2, pp. 4–12, 2012.

[39] I. G. Insua, *Optical generation of mm-wave signals for use in broadband radio over fiber systems*. Jörg Vogt Verlag, 2010.

[40] J. O'reilly, P. Lane, R. Heidemann, and R. Hofstetter, "Optical generation of very narrow linewidth millimetre wave signals," *Electronics Letters*, vol. 28, pp. 2309–2311, 1992.

[41] S. Ghafoor and L. Hanzo, "Reduced dispersion duplex dqpsk radio-over-fiber communications using single-laser-based multiple side-bands," in *2011 IEEE International Conference on Communications (ICC)*, pp. 1–5, IEEE, 2011.

[42] A. Bogoni and A. Willner, "Photonic signal processing for logic and computation," in *All-Optical Signal Processing*, pp. 157–183, Springer, 2015.

[43] R. L. Abrams and R. C. Lind, "Degenerate four-wave mixing in absorbing media," *Opt. Lett*, vol. 2, no. 4, pp. 94–96, 1978.

[44] R. Welstand, S. Pappert, C. Sun, J. Zhu, Y. Liu, and P. Yu, "Dual-function electroabsorption waveguide modulator/detector for optoelectronic transceiver applications," *IEEE Photonics Technology Letters*, vol. 8, no. 11, pp. 1540–1542, 1996.

[45] L. Noel, D. Wake, D. Moodie, D. Marcenac, L. Westbrook, and D. Nesset, "Novel techniques for high-capacity 60-ghz fiber-radio transmission systems," *IEEE Transactions on microwave theory and techniques*, vol. 45, no. 8, pp. 1416–1423, 1997.

[46] J.-S. Wu, J. Wu, and H.-W. Tsao, "A radio-over-fiber network for microcellular system application," *IEEE transactions on vehicular technology*, vol. 47, no. 1, pp. 84–94, 1998.

[47] A. Stohr, K.-i. Kitayama, and D. Jager, "Full-duplex fiber-optic rf subcarrier transmission using a dual-function modulator/photodetector," *IEEE transactions on microwave theory and techniques*, vol. 47, no. 7, pp. 1338–1341, 1999.

[48] A. Nirmalathas, D. Novak, C. Lim, and R. B. Waterhouse, "Wavelength reuse in the wdm optical interface of a millimeter-wave fiber-wireless antenna base station," *IEEE Transactions on Microwave Theory and Techniques*, vol. 49, no. 10, pp. 2006–2012, 2001.

[49] M. Bakaul, A. Nirmalathas, and C. Lim, "Multifunctional wdm optical interface for millimeter-wave fiber-radio antenna base station," *Journal of lightwave technology*, vol. 23, no. 3, p. 1210, 2005.

[50] Z. Jia, J. Yu, and G.-K. Chang, "A full-duplex radio-over-fiber system based on optical carrier suppression and reuse," *IEEE Photonics Technology Letters*, vol. 18, no. 16, pp. 1726–1728, 2006.

[51] J. Yu, Z. Jia, T. Wang, and G.-K. Chang, "A novel radio-over-fiber configuration using optical phase modulator to generate an optical mm-wave and centralized lightwave for uplink connection," *IEEE Photonics Technology Letters*, vol. 19, no. 3, pp. 140–142, 2007.

[52] Y.-Y. Won, H.-C. Kwon, and S.-K. Han, "1.25-gb/s wavelength-division multiplexed single-wavelength colorless radio-on-fiber systems using reflective semiconductor optical amplifier," *Journal of Lightwave Technology*, vol. 25, no. 11, pp. 3472–3478, 2007.

[53] J. V. Olmos, T. Kuri, and K.-i. Kitayama, "Dynamic reconfigurable wdm 60-ghz millimeter-waveband radio-over-fiber access network: architectural considerations and experiment," *Journal of Lightwave Technology*, vol. 25, no. 11, pp. 3374–3380, 2007.

[54] M.-F. Huang, J. Yu, Z. Jia, and G.-K. Chang, "Simultaneous generation of centralized lightwaves and double/single sideband optical millimeter-wave requiring only low-frequency local oscillator signals for radio-over-fiber systems," *Journal of Lightwave Technology*, vol. 26, no. 15, pp. 2653–2662, 2008.

[55] H.-C. Ji, H. Kim, and Y. C. Chung, "Full-duplex radio-over-fiber system using phase-modulated downlink and intensity-modulated uplink," *IEEE Photonics Technology Letters*, vol. 21, no. 1, pp. 9–11, 2009.

[56] A. Chowdhury, H.-C. Chien, Y.-T. Hsueh, and G.-K. Chang, "Advanced system technologies and field demonstration for in-building optical-wireless network with integrated broadband services," *Journal of lightwave technology*, vol. 27, no. 12, pp. 1920–1927, 2009.

[57] V. A. Thomas, S. Ghafoor, M. El-Hajjar, and L. Hanzo, "A full-duplex diversity-assisted hybrid analogue/digitized radio over fibre for optical/wireless integration," *IEEE Communications Letters*, vol. 17, no. 2, pp. 409–412, 2013.

[58] T. Kuri, T. Nakasyotani, H. Toda, and K.-I. Kitayama, "Characterizations of supercontinuum light source for wdm millimeter-wave-band radio-on-fiber systems," *IEEE photonics technology letters*, vol. 17, no. 6, pp. 1274–1276, 2005.

[59] T. Nakasyotani, H. Toda, T. Kuri, and K.-i. Kitayama, "Wavelength-division-multiplexed millimeter-waveband radio-on-fiber system using a supercontinuum light source," *Journal of lightwave technology*, vol. 24, no. 1, p. 404, 2006.

[60] Y.-T. Hsueh, Z. Jia, H.-C. Chien, J. Yu, and G.-K. Chang, "A novel bidirectional 60-ghz radio-over-fiber scheme with multiband signal generation using a single intensity modulator," *IEEE photonics technology letters*, vol. 21, no. 18, pp. 1338–1340, 2009.

[61] S. Ghafoor, V. A. Thomas, and L. Hanzo, "Duplex digitized transmission of 64-qam signals over a single fiber using a single pulsed laser source," *IEEE Communications Letters*, vol. 16, no. 8, pp. 1312–1315, 2012.

[62] Z. Tang and S. Pan, "A full-duplex radio-over-fiber link based on a dual-polarization mach–zehnder modulator," *IEEE Photonics Technology Letters*, vol. 28, no. 8, pp. 852–855, 2016.

[63] N. Pleros, K. Tsagkaris, and N. D. Tselikas, "A moving extended cell concept for seamless communication in 60 ghz radio-over-fiber networks.," *IEEE Communications Letters*, vol. 12, no. 11, pp. 852–854, 2008.

[64] P. Monteiro, S. Pato, E. López, D. Wake, N. J. Gomes, and A. Gameiro, "Fiber optic networks for distributed radio architectures: Futon concept and operation," in *Wireless Communications and Networking Conference Workshops (WCNCW), 2010 IEEE*, pp. 1–5, IEEE, 2010.